TARADCOM

R and D LABORATORY

TECHNICAL REPORT

NO. 12380

TRACK-SOIL INTERACTION MODEL FOR THE DETERMINATION OF MAXIMUM SOIL THRUST

by Leslie L. Karafiath

Research Department
Grumman Aerospace Corporation
Bethpage, New York 11714

Contract DAAE07-75-C-0066
Amendments P0004-P0008

U.S. ARMY TANK-AUTOMOTIVE
RESEARCH AND DEVELOPMENT COMMAND
Warren, Michigan 48090

RE-556

TRACK-SOIL INTERACTION MODEL FOR THE DETERMINATION OF MAXIMUM SOIL THRUST

Final Report No. 12380

by

Leslie L. Karafiath

Prepared Under Contract DAAE07-75-C-0066

Amendments P0004-P0008

for

U.S. Army Tank-Automotive Research
and Development Command
Warren, Michigan 48090

by

Research Department
Grumman Aerospace Corporation
Bethpage, New York 11714

July 1978

Approved by: John T. Graham
for Richard A. Scheuing
Director of Research

FOREWORD

Recent developments in defensive weapons systems make it imperative for the combat and support vehicles of the Army to move on the ground with utmost agility. In the case of tracked vehicles, the acceleration needed for off-road agility is often limited by the soil thrust that the track can develop. The soil thrust provides the traction needed to overcome motion resistance and provides the accelerating force as well. This accelerating force is resisted by an equal and opposite intertial force acting at the CG of the vehicle. The resulting moment is balanced by a redistribution of the interface normal stresses that, in turn, affect the soil thrust that can be developed and the trim angle of the vehicle. Thus, the maximum soil thrust, the accelerating force, the distribution of interface normal stresses and the trim angle are interrelated. The present, largely empirical methods estimate the performance of tracked vehicles traveling at a constant speed and are not directly applicable to problems involving track-soil interaction at times of acceleration.

In the case of turning, the soil thrust developed by the outer track provides the slewing force needed to overcome the turning resistances. All of these forces act at the level of the track-soil interface and, therefore, do not affect the moment equilibrium about the CG of the vehicle. The distribution of interface normal stresses computed for these conditions is the basis for the determination of shear resistances that oppose lateral movement of the tracks during skid steering.

The applied mechanics approach developed at Grumman over the years for the solution of wheel-soil and tire-soil interaction problems is applied to these track-soil interaction problems. In this approach the track is considered as a free body, and the interaction problem is resolved by determining the stresses acting on the interface of track and soil. In the limiting case of maximum soil thrust, the applied track forces generate shear stresses that cause the soil to fail under the track load. For determining the stress state of the soil under these conditions, the soil is characterized by its Coulomb strength parameters, and the methods of plasticity theory are applied. The analytical model of track-soil interaction developed by using this approach is suitable for the parametric

analysis of the effect of various design variables on acceleration performance and offers insight into the interrelationships that govern that acceleration performance.

ABSTRACT

An analytical track-soil interaction model has been developed for the determination of maximum soil thrust. The model assumes rigid track geometry characterized by the dimensions of the main ground contact area and the approach angle. The position of the track is defined by its trim angle and sinkage at the front. Limits of interface stresses are determined by assuming soil failure in either the longitudinal or transverse direction. Within these limits adjustments are made to meet the requirement of moment equilibrium about the CG. The maximum soil thrust is determined by the interface stress distribution that satisfies equilibrium and allows the development of the highest interface friction angle. Results of parametric analyses obtained by the model regarding the effect of track length/width ratios and CG locations on acceleration performance are shown.

A semirigid track-tire interaction model has also been developed. This model shows that in soft soil the acceleration performance of pin-jointed tracks is governed by the interaction of the soil beneath the last roadwheel and the most rearward track links. Several concepts, aimed at improving the acceleration performance of tracked vehicles, are presented.

Turning resistances comprise shear resistances arising at the track-soil interface and passive earth resistances arising at the side faces of tracks. These are analyzed and methods are presented for their computation.

ACKNOWLEDGEMENT

The work reported herein was performed for the Tank-Automotive Concepts Laboratory of the U.S. Army Tank-Automotive Research and Development Command (TARADCOM), Warren, Michigan, under the general supervision of Dr. Jack Parks, Director of the Laboratory, Mr. Otto Renius, Chief, Survivability Research Division, and Mr. Zoltan J. Janosi, Chief, Applied Research Function. Mr. Zoltan J. Janosi was also technical monitor. Their help and valuable suggestions in carrying out this work are gratefully acknowledged.

TABLE OF CONTENTS

LIST OF ILLUSTRATIONS

1. SCOPE OF WORK AND OBJECTIVES

The scope of work and objectives of the program include the following items:

- Development of a track-soil interaction model for the determination of maximum soil thrust
- Development of a track-soil interaction model for the analysis of the effect of the location of the CG on acceleration performance
- Analysis of lateral slip and passive resistances developing at the side of the track during turning

2. CONCEPT OF TRACK-SOIL INTERACTION

The fundamental concept applied to the solution of track-soil interaction problems described in the Scope of Work is that the interaction problem is resolved if, considering the track as a free body, the stresses at its interface with the soil are determined. Application of this principle to track-soil interaction problems in general leads to the need for stress and displacement calculations in the elastic-plastic state of the soil. While it would be desirable to develop a track-soil interaction model for these conditions (using nonlinear finite element methods), at the present state of the art of the determination of soil properties in mobility research, the input parameters necessary for such nonlinear analyses would not be obtainable. Since at the limit of track performance the plastic behavior of soil (characterized by its Coulomb strength parameters) governs track-soil interaction, the present discussion is centered on the limiting cases.

The interface normal stresses associated with the plastic state of failure in the soil constitute a limit for the normal stresses that must not be exceeded. The magnitude of these limiting normal stresses depends not only on the strength properties of soil, but also on the applied tangential force; the higher the tractive (tangential) force the lower the limiting interface normal stress. The vertical components of all interface stresses must equal the track load; the limiting normal stress distribution that corresponds to the largest tractive force while still maintaining load equilibrium is the critical one and yields the maximum soil thrust. In this case, the limiting normal stresses are associated with soil failure in the plane of travel. However, in the case of tracks, another mode of soil failure in the plane perpendicular to the plane of travel is also possible. To decide which mode of failure should be considered for determining interface stresses, the following principle is postulated:

> Of all the potential planes passing through a point of the track-soil interface in which soil failure is possible, the one yielding the lowest normal stress at that point is the valid one.

Applying this principle to track-soil interaction problems means that for the calculation of limiting normal stresses both longitudinal and transverse failure conditions have to be considered.

The characterization of soil behavior by its Coulomb strength parameters is satisfactory for the determination of the plastic state of stresses in the soil corresponding to given stress and geometric boundary conditions. However, such characterization by itself is insufficient for the determination of the sinkage associated with the plastic state of stresses in the soil. In the case of a rigid wheel or pneumatic tire, the change in the contact area with sinkage is so overpowering that contact area requirements control sinkage. In the case of tracks, there is but little change in the contact area with sinkage and, therefore, sinkage is governed by the volume change properties of soil rather than by changes in the contact area. Consequently, for the proper formulation of track-soil interaction, it is necessary to introduce some additional descriptors for the characterization of the volume change properties of soil.

The sinkage associated with the development of plastic failure zones beneath a loaded area may be computed if the void ratio of the in-situ soil is known, and the void ratio at failure has been determined by appropriate triaxial tests. For the purpose of the prediction of sinkage of tracked vehicles it is more expedient to use a descriptor of volume changes that may be determined by field methods used in off-road vehicle engineering. Plastic failure zones develop in a plate sinkage test; the sinkage associated with the development of these failure zones is a measure of the volume changes and may be used to characterize the volume change properties of soil.

In a plate sinkage test, the complete development of failure zones, or bearing capacity, is reached when the tangent of the pressure-sinkage curve (Fig. 1)

$$\frac{dp}{dz} = \gamma s_q Nq \qquad (1)$$

where γ = unit weight of soil

s_q = shape factor

Nq = bearing capacity factor.

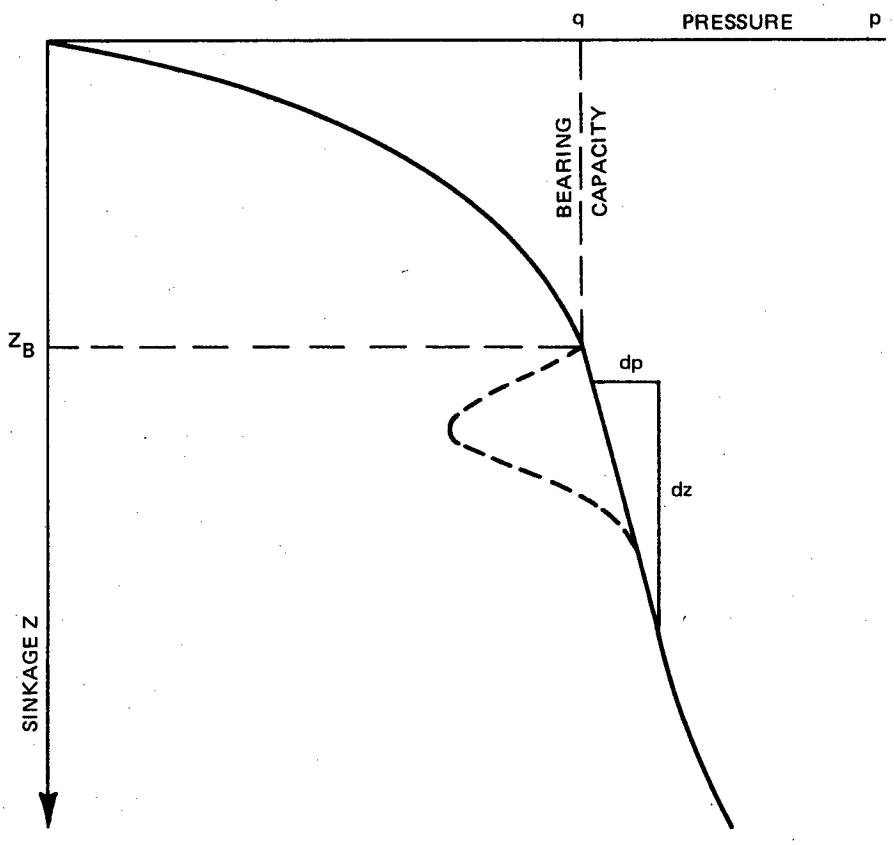

Fig. 1 Determination of the Sinkage at Bearing Capacity Failure (Z_B) from Pressure Sinkage Curve Obtained in Plate Sinkage Test

The sinkage at bearing capacity, Z_B, is a measure of the volume changes that occur in the soil as plastic failure zones develop. In dimensionless form, the sinkage at bearing capacity may be expressed as follows:

$$Z_B = K_B s_B \sqrt{A} \tag{2}$$

where A = area of plate

K_B = coefficient of sinkage

s_B = shape factor (=1 for square or circular areas)

The coefficient of sinkage is the additional parameter needed to predict sinkage in track-soil interaction. It may be determined by plate sinkage tests or its value may be estimated from experience.

In formulating the relationships that govern track-soil interaction, the modeling of the track geometry plays an important role. Pin-jointed tracks used generally on military vehicles are flexible in both upward and downward directions. An ideal modeling of the track geometry would be that by the coordinates of the pins constrained only by the requirement that the distance between adjacent pins is constant. However, in the first stage of model development the track is assumed to be rigid, characterized by its main dimensions and the approach angle. Interactions due to the relative displacements of track links are disregarded. Even though the assumption of a rigid track means that it is uncoupled from the suspension system, it is essential to consider the interactions involving the CG of the vehicle. There is an interaction between an accelerating soil thrust (balanced by an equal and opposite inertial force acting on the CG) and the distribution of interface normal stresses.

For the determination of maximum soil thrust it is essential to take this interaction into account and to assume that the rigid track is rigidly coupled to a hypothetical CG assumed to be in the vertical plane of the longitudinal axis of the track.

The assumption of a rigid track geometry greatly simplifies computations, but is deficient in representing the track behavior realistically. Analyses, performed by means of the rigid track model and reported later in this report, showed that important aspects of track-soil interaction remain obscured because of this assumption. The development of a flexible track

model that would realistically simulate the effects of track flexibility is outside the scope of this contract. A semirigid track-soil interaction model, developed as a first step toward taking into accound the effect of track flexibility on soil response and described in Section 4, clearly shows that in a rigid track-soil interaction model the soil response is unduly influenced by the assumption of rigidity, and a track model that takes track link movements into account is needed for the realistic simulation of track-soil interaction.

3. AN ANALYTICAL RIGID TRACK-SOIL INTERACTION MODEL FOR THE DETERMINATION OF MAXIMUM SOIL THRUST

In this model the track is assumed to be rigid. The geometry of the track is characterized by the length of the main ground contact area (L) and the approach angle (α). The width of the track (B) is constant. The position of the track is determined by the front sinkage (Z_f) and trim angle (λ) (Fig. 2). The CG of the vehicle is defined by its height over the ground contact area, h_c, and the distance from the rear end of the ground contact area, X_c. For the purpose of the modeling of track-soil interaction, the CG is assumed to be in the vertical plane of symmetry bisecting the width of the track.

The soil is modeled by its Coulomb strength parameters and sinkage coefficient. For the determination of interface stresses acting on the main track area, both longitudinal and transverse failure conditions are considered (Fig. 3). The geometry of the slip line field for longitudinal failure depends on the Coulomb strength parameters of the soil, the trim angle, and the interface friction angle. The slip line field for transverse failure is computed on the assumption that no shear stresses develop in the transverse direction beneath the track. The geometry of the slip line field for transverse failure and the interface stresses computed therefrom vary with the depth of the track beneath the original surface. To determine whether longitudinal or transverse failure conditions govern the interface stresses beneath any particular point of the track, the criterion discussed in Section 2 is applied. The interface normal stress is computed for both conditions, and whichever yields the lower normal stress is the valid limiting condition at that point.

For computational purposes a grid system is established over half of the main track area (Fig. 4). First, the interface normal stresses corresponding to longitudinal failure are computed by numerical integration of the differential equations of plasticity for soils. Computational routines for this differ but little from those used with tire-soil and wheel-soil interaction problems (Refs. 1 and 2). However, it was found more expedient to use the scheme with a constant rather than a variable number of "j" lines. The grid system shown in Fig. 4 is equidistant, whereas the slip

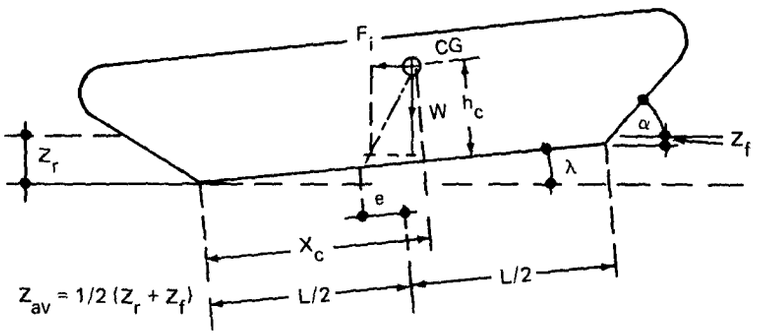

Fig. 2 Assumed Track Geometry

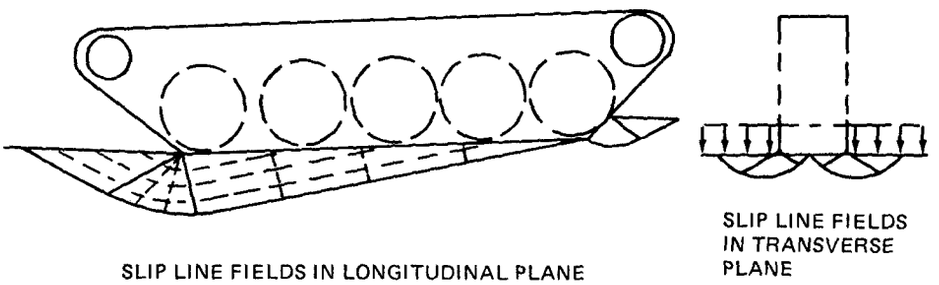

Fig. 3 Slip Line Fields Considered for the Determination of Interface Stresses

line field yields normal stresses at locations that depend on the slip line field geometry and, therefore, are not equidistant. An interpolation scheme is used that determines the normal stresses at the equidistant grid points in the longitudinal direction. Under these circumstances a constant number of "j" lines is desirable for both the ease and accuracy of the interpolation.

In regard to failure in the longitudinal direction, conditions are the same along any n = constant line. Thus, the normal stresses computed for say n = 1 are valid for any other n value in the grid.

In the transverse direction the depth at various "m" locations varies and, therefore, the normal stresses are computed for each location separately. Again, the slip line field computation yields the normal stresses at intersections of the "j" lines with the track surface. These are not equidistant, and the use of an interpolation scheme is necessary to determine the normal stresses at the equidistant grid points. The normal stresses computed from the two schemes of the grid points are compared, and whichever is lower is retained for further computations.

The slip line fields considered for the determination of interface stresses acting on the front inclined portion of the track are shown in Fig. 5. In the transverse direction it is assumed that the front portion consists of steps, instead of a continuous incline. Failure is assumed to occur in the vertical plane. The vertical normal stresses obtained on the step faces are then resolved into components normal and tangential to the incline. These normal stresses are then compared with those computed for longitudinal failure in a similar way to that for the main track area.

In connection with the longitudinal slip line field shown in Fig. 5, it is necessary to establish a relationship between the interface friction angle, δ, acting at the main ground contact area of the track and that acting at the inclined front portion (ramp) of the track (δ_r). Application of the concept of kinematic boundary conditions brought forth in Ref. 3 for pneumatic tires to the assumed track geometry results in the following relationships (Fig. 6): According to this concept the directions of the major principal stress, σ_1, and the velocity vector, $\bar{v}_r$, coincide. From the vector diagram in Fig. 6, the following relation holds

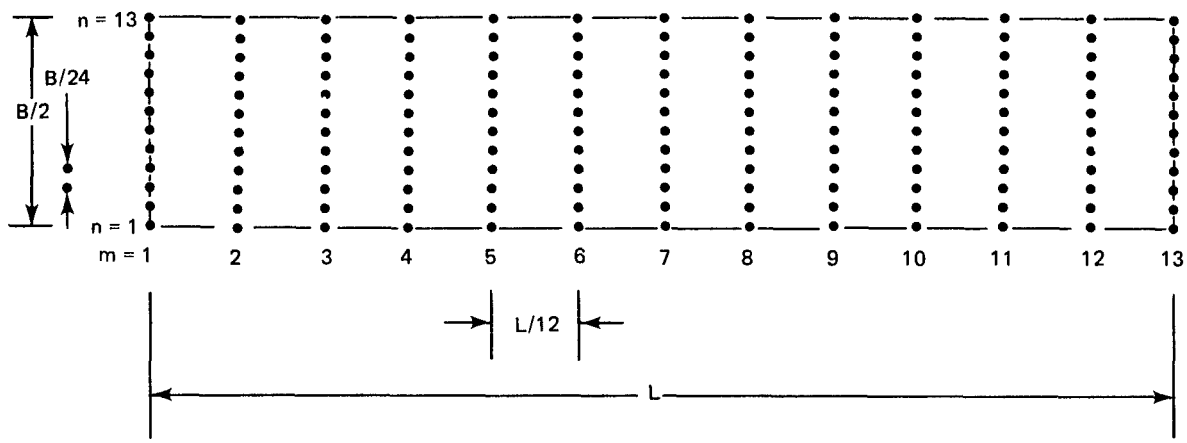

Fig. 4 Grid System for the Computation of Interface Normal Stresses Beneath the Main Track Area (B = Width of Track)

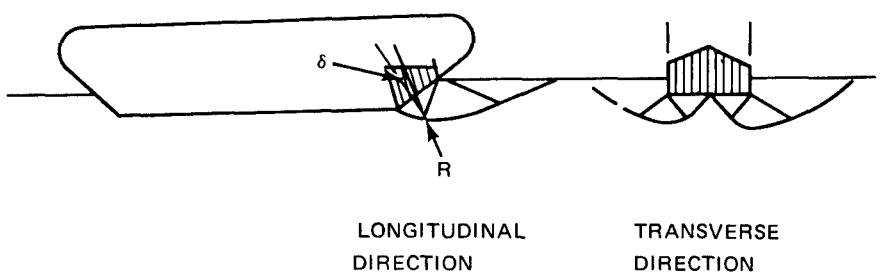

Fig. 5 Slip Line Field for the Determination of Interface Stresses Acting on the Front Inclined Portion of Track

$$\tan \theta_r = \frac{\sin(\alpha+\lambda) \sin \theta_m}{\sin(\lambda+\theta_m) - \cos(\alpha+\lambda) \sin\theta_m} \tag{3}$$

where θ_r, θ_m are the directions of the resultant velocity vectors, $(\bar{v}_r)$, coinciding with the direction of the major principal stress, σ_1, at the ramp and at the main track area, respectively.

The θ angles are related to the δ angles by the following equation

$$\theta = \frac{\pi}{2} - \Delta - \delta \tag{4}$$

where $\Delta = \arcsin \frac{\sin\delta}{\sin\phi}$

ϕ = friction angle

While θ_r defines δ_r at the ramp, the equations cannot be directly resolved for δ_r; therefore, an iterative approximation to solve for δ_r has been devised.

The computation of interface stresses for sample cases showed that in certain cases the normal stress beneath the front end of the main track area computed for a forward failure is less than that computed for a slip line field assumed beneath the main track area and shown in Fig. 3. Therefore, the slip line field computation, originally devised for the determination of the interface stresses acting on the ramp area only, has been modified to cover part of the main track area too. Figure 7 shows such a modified slip line field. The interface normal stresses computed for the front portion of the main track area from this extended slip line field are compared with those computed from the longitudinal and transverse slip line fields beneath the main track area; whichever normal stress is lower is retained as the valid limiting normal stress.

The procedures described before are suitable for the determination of interface stresses for a given sinkage and trim angle and an assumed interface friction angle, δ. The summation of the vertical components of the interface stresses yields the load. If the track load is given, an iteration on δ is necessary to bring about the equilibrium of vertical forces. The δ angle at which the vertical forces balance is the maximum that can be applied; the summation of horizontal components of interface

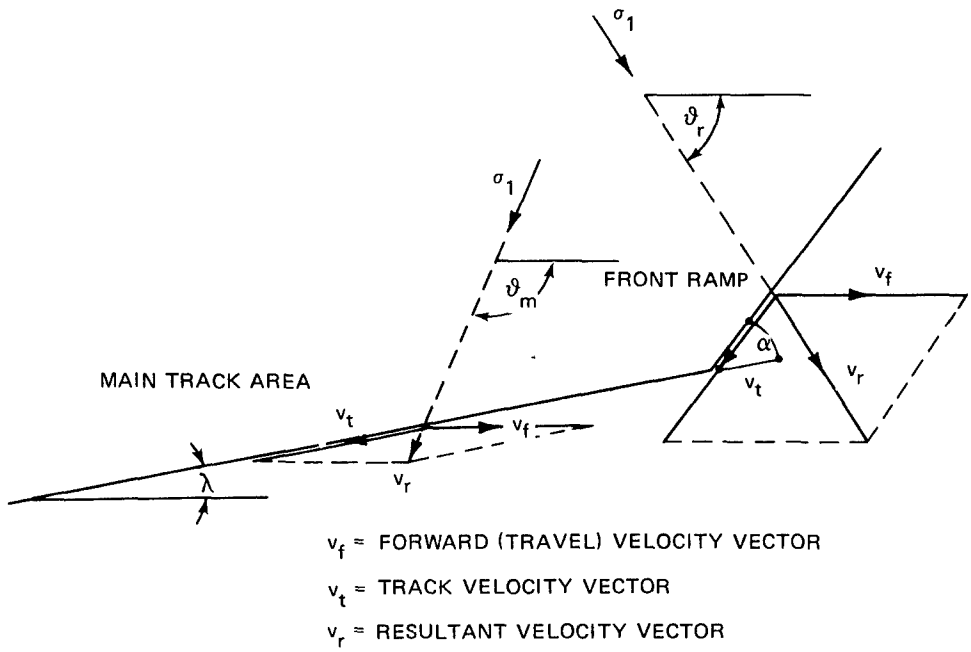

Fig. 6 Kinematic Boundary Conditions at the Track-Soil Interface

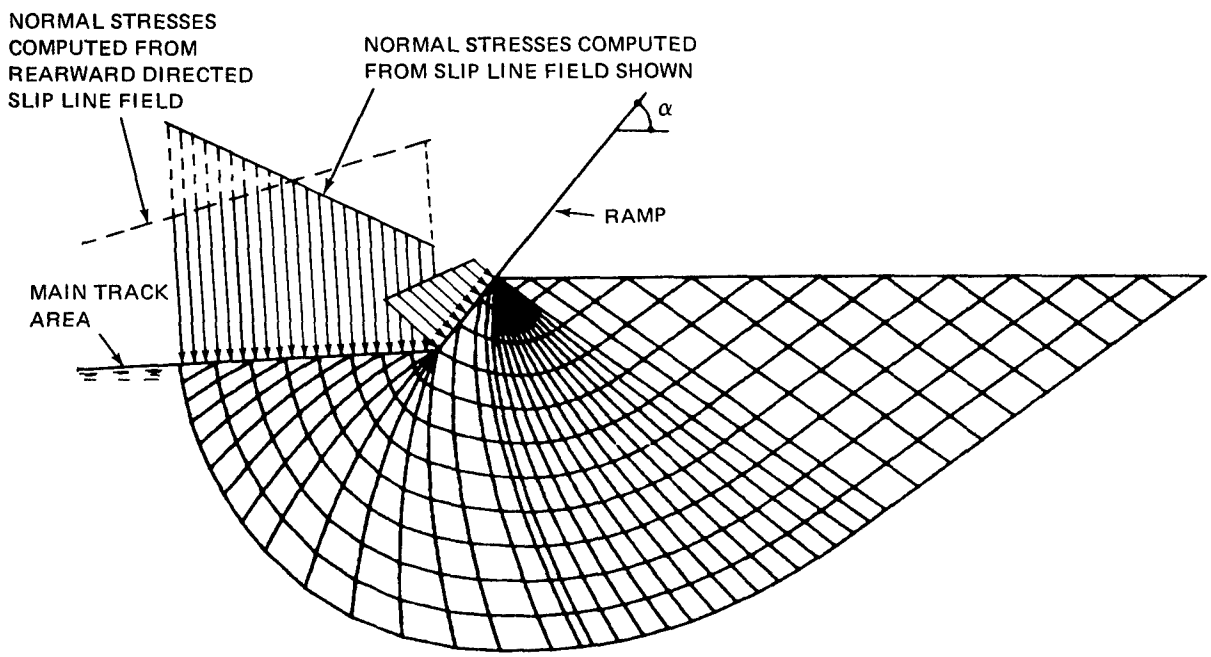

Fig. 7 Front Slip Line Field modified to Include Part of the Main Track Area

stresses yields the maximum soil thrust. Note that at this point the moment equilibrium about the CG is not necessarily satisfied. The interface friction angle, δ, associated with a distribution of interface normal stresses that satisfies the vertical force equilibrium, is designated as δ_{vlim}.

For prediction purposes, it is necessary to estimate the sinkage and the trim angle. In Section 2 the concept of sinkage coefficient was introduced. For the estimation of track sinkage the shape factor in Eq. (2) must be known. This shape factor is not identical to that used in various bearing capacity equations for consideration of the effect of shape on bearing capacity, since the shape factor in Eq. (2) applies to the sinkage associated with the development of failure zones at bearing capacity. Since experimental information on the sinkage of plates of various shapes has been found scanty and insufficient for the derivation of an empirical correlation for the estimation of the shape factor, s_B, theoretical analyses have been performed. Bearing capacities of plates with various aspect ratios have been determined by the same method as described before for the determinaton of track-soil interface stresses. Furthermore, it has been assumed that the following logarithmic relationship exists between the void ratio at failure and the major principal stress:

$$e_f - e_o = C_f \log \sigma_{1f}/\sigma_{1o} \tag{5}$$

where e_o = initial void ratio

e_f = void ratio at failure

C_f = coefficient of volume change

σ_{1f} = major principal stress at failure

σ_{1o} = initial major principal stress

Using this equation for the determination of volume changes, sinkage computations were made for a wide range of initial void ratios and C_f coefficients. Results of these computations are shown in Fig. 8. It has been found that the following equation yields a reasonably good approximation

$$s_B = 1/(0.1R_a + 0.9) \tag{6}$$

where R_a = aspect ratio = width/length.

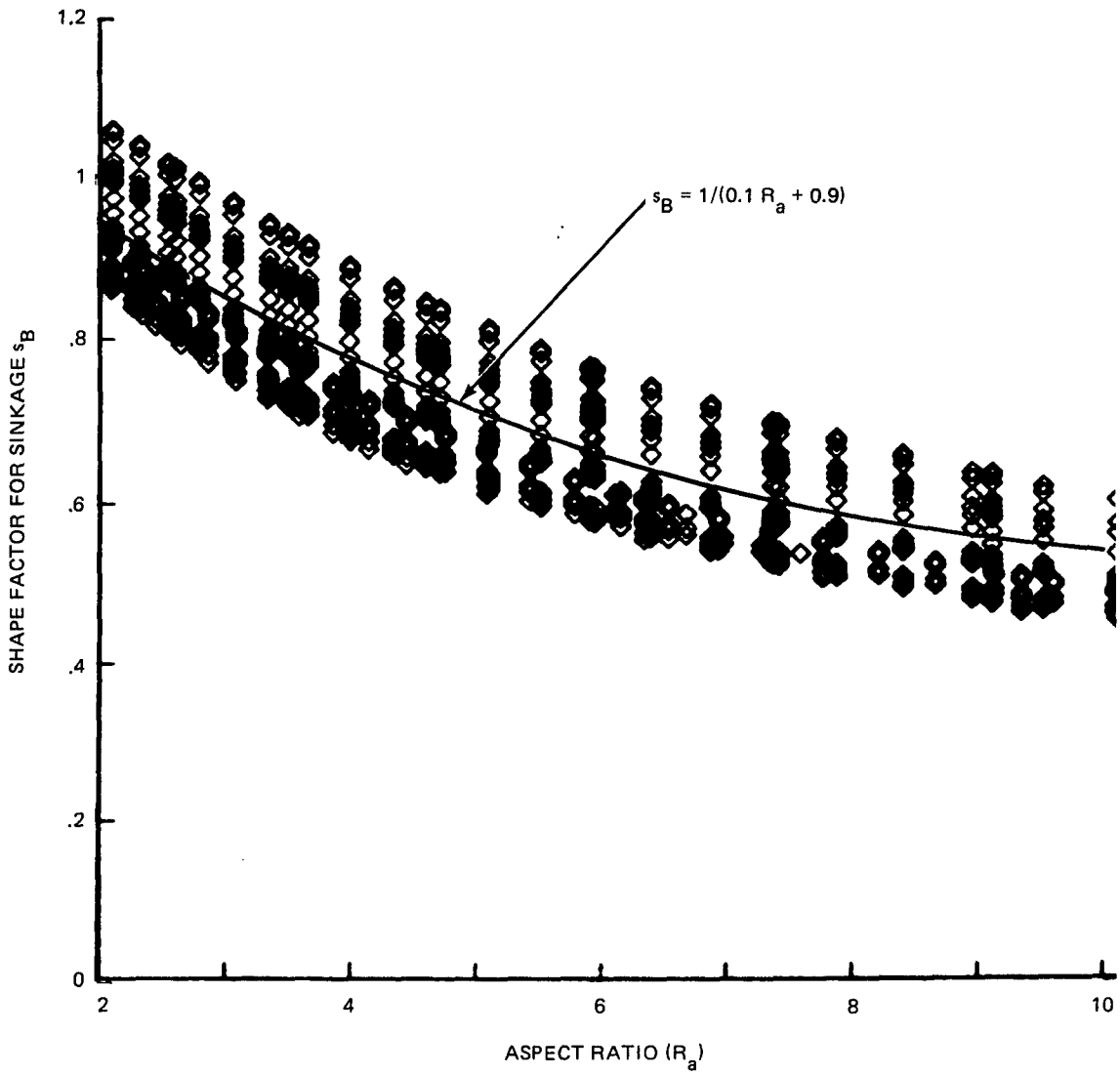

Fig. 8 Shape Factors Computed for a Variety of Initial Void Ratios, Volume Change Coefficients and Aspect Ratios

For the estimation of the trim angle it is assumed that at an eccentricity of L/6 the sinkage at the front is zero and at the rear it is twice the average sinkage. For other eccentricities, the trim angle, λ, is calculated from the following formula:

$$\tan \lambda = 12e.z_{av}/L^2 \qquad (7)$$

where e = eccentricity

L = length of ground contact area

The tractive force that accelerates the vehicle is balanced by an inertial force acting at the CG of the vehicle. The moment generated by this force couple is balanced by a redistribution of the normal stresses requiring their resultant to act at some distance rearwards from the CG. Obviously, such a redistribution requires that the normal stresses be reduced in the front and increased in the rear. A reduction of the normal stresses in the front means that the normal stresses there will be of a lesser magnitude than those causing failure. To compensate for the reduction of the normal stresses in the front, they must be increased in the rear so that the vertical force equilibrium is maintained. Any increase in the normal stresses would, of course, exceed the limit shown in the upper part of Fig. 9 and computed for $\delta = \delta_{vlim}$. Thus, it is necessary to adjust δ so as to allow for the necessary increase of normal stresses in the rear portion of the track.

In the lower part of Fig. 9, the schematics of redistribution of the normal stresses are shown. A new limit for the interface normal stresses is computed for $\delta < \delta_{vlim}$. It is assumed that the redistributed normal stresses vary linearly. Subsequent reductions are tentatively assumed as shown in the lower part of Fig. 9 by the numbered lines. The vertical force equilibrium is checked subsequently for each of these lines; when the vertical force equilibrium is satisfied, the moment equilibrium is checked. If there is an unbalanced moment greater than the allowed tolerance, δ is adjusted and the procedure repeated until an interface normal stress distribution is found that satisfies both the vertical force and moment equilibrium conditions. The interface friction angle that pertains to this distribution is $\delta = \delta_{max}$, $(< \delta_{vlim})$, the highest that can be developed for maximum soil thrust.

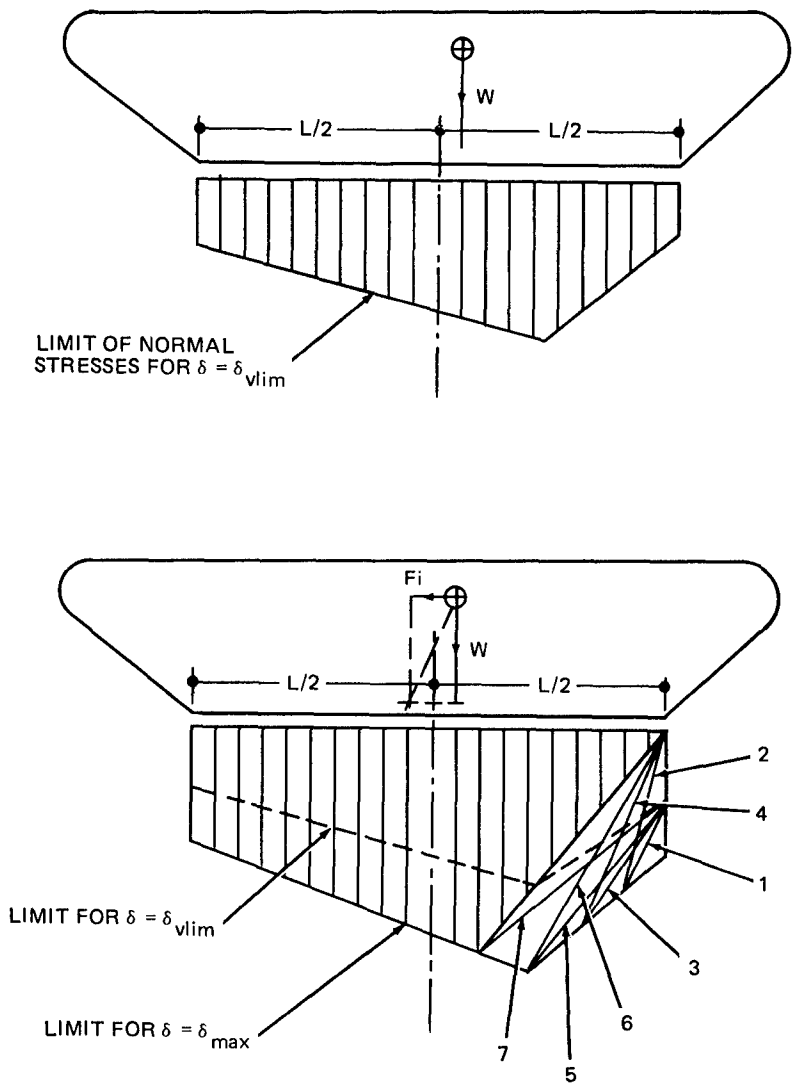

Fig. 9 Schematic of Distribution and Redistribution of Interface Normal Stresses

Results of parametric analyses performed with the rigid track-soil interaction model are presented in Section 5. In the course of these analyses it has become apparent that the necessity of satisfying the moment equilibrium often requires a quite appreciable redistribution of the interface normal stresses. As a result of redistribution the normal stresses along a significant length of the track in the front part are less than the limiting normal stresses associated with the plastic state of stresses in the soil. The question arises how well this redistribution of interface normal stresses simulates the actual conditions. In the case of girderized tracks, the rigid track geometry assumed in the model approximates the behavior of the track closely, and the predicted redistribution of normal stresses is reasonable. However, in the case of pin-jointed tracks used by the military, the flexibility of the track alters the stress distribution, and the simulation assuming a rigid track model becomes unrealistic. In the endeavor to solve this problem, a tentative model has been developed as an alternate. This model is discussed in Section 4.

4. CONCEPT OF SEMIRIGID TRACK-SOIL INTERACTION MODEL

Pin-jointed, flexible tracks transmit load to the soil in a manner fundamentally different from the way rigid tracks do. Generally, in a pin-jointed track there are some four to six links per roadwheel contacting the ground. Depending on the instantaneous track configuration relative to the roadwheels, some of these links are loaded directly by a roadwheel and assume a concave configuration. These links then load the soil directly and, if traction is applied, obliquely. With increasing traction, plastic failure zones tend to develop in the soil, the sinkage of the loaded links increases, and the soil is pushed rearward from beneath the loaded links. At this point the links that are in between roadwheels but not in contact with them play a counterbalancing role by resisting the upward push of the soil. In soil mechanics terms the soil immediately beneath the links loaded by a roadwheel is in the active state of pressure, while underneath the other links to the rear it is in the passive state. The restraining pressure exerted by these latter links also allows the development of higher stresses beneath the directly loaded links. A slip line field solution for the plastic equilibrium conditions obtained beneath a section of a pin-jointed track is shown in Fig. 10.

The sample slip line field shown in Fig. 10 has been obtained for arbitrarily assumed conditions by trial and error method. Generally, the lengths of the active and passive zones do not match an even number of links. Also, the restraining pressures acting on the passive zone as well as the interface friction angles acting at each link have been arbitrarily assumed. The development of a model where the equilibrium condition of each link, the conditions of plastic equilibrium in the soil, and the overall equilibrium conditions are satisfied is an extremely difficult task, and outside of the scope of this work. Nevertheless, the development of a preliminary model has been initiated -- primarily to evaluate the implications of assuming a rigid geometry for pin-jointed tracks.

To simplify the complexities of flexible track-soil interaction, it has been assumed for this preliminary model development that the links directly loaded by the roadwheels behave as rigid bodies, and the action

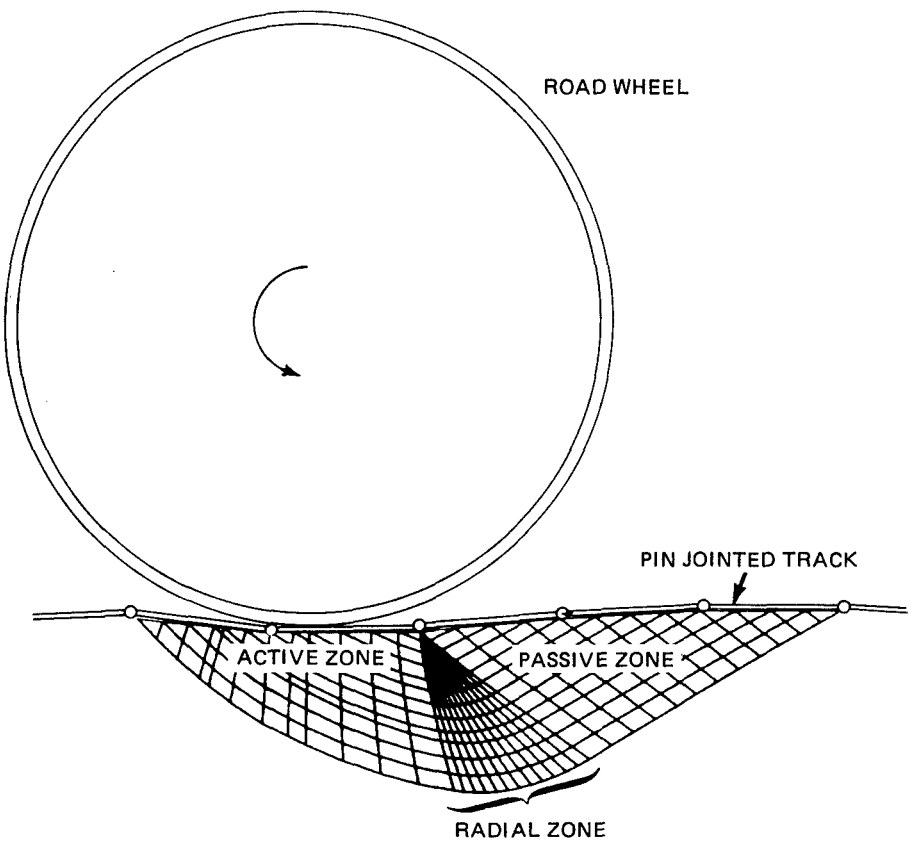

Fig. 10 Slip Line Field Beneath a Section of a Pin-Jointed Track

of the nondirectly loaded links is equivalent to a surcharge (Fig. 11). Thus there is a rigid loaded area beneath each roadwheel; the longitudinal dimension of the loaded area equals three link lengths beneath the first and last roadwheel and two link lengths elsewhere. The first link underneath the first roadwheel inclines at the approach angle. All other links are assumed to be in the same plane -- that is, inclined at the trim angle to the horizontal.

The computation of the interface stresses beneath each loaded area is similar to that described for the rigid track model in Section 3. At this stage of the development, however, the inertial force due to acceleration has to be assumed so that the load on each roadwheel and the trim angle associated with the eccentricity of the load may be computed.

At the present stage of development this semirigid model of track-soil interaction represents only a very crude approximation of the actual effect of track flexibility. Nevertheless, some interesting results obtained with the semirigid track-soil interaction model are worth mentioning since rigid models tend to obscure the significance of some of the design characteristics of tracks that are particularly important for agility. These results are:

- For acceleration in soft soil, the critical component of the track-soil system is the last roadwheel. At times of acceleration the load on this roadwheel is increased due to load transfer, yet from the viewpoint of soil supporting capacity the last roadwheel is the weakest link in the track-suspension-soil system. The tractive force tends to push the soil out backwards from underneath the loaded links; the links that are not directly loaded resist this push everywhere but at the last roadwheel. Thus, the interaction between the track beneath the last roadwheel and the soil is critical for acceleration in soft soil
- The roadwheels load the soil directly over an area the dimension of which in the longitudinal direction is determined by the length of the links (pitch) in a pin-jointed track

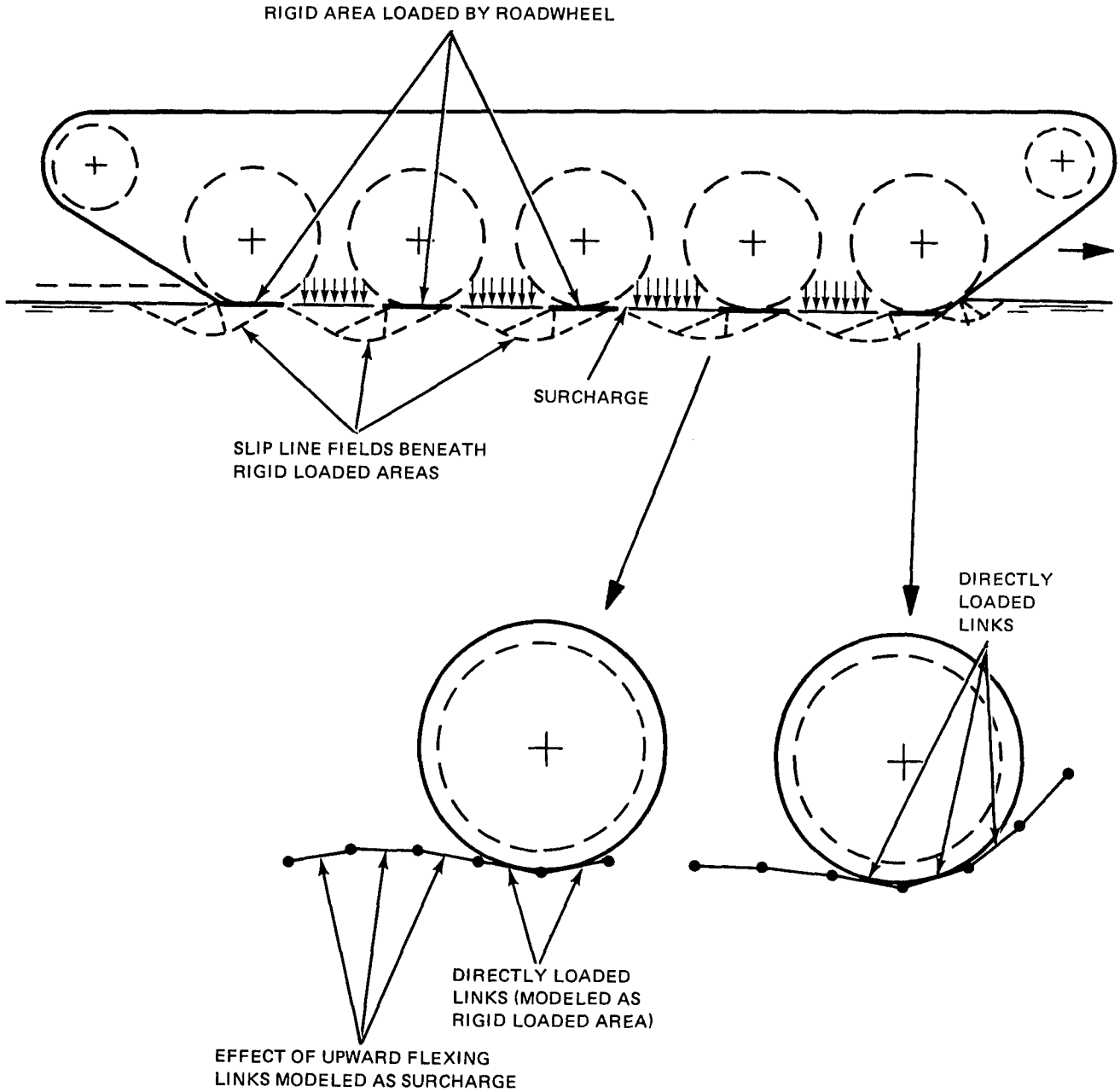

Fig. 11 Concept of Semirigid Track-Soil Interaction Model

Since the bearing capacity of soil increases with the dimensions of the loaded area, greater link length results in improved acceleration performance in soft soils

Results of sample acceleration predictions by the semirigid track-soil interaction model are presented in Section 5.

5. RESULTS OF ANALYSES PERFORMED BY THE TRACK-SOIL INTERACTION MODELS

The track-soil interaction model developed for the determination of maximum soil thrust is suitable for the analysis of the effect of various design variables on the maximum soil thrust. This analytical capability of the model is an essential tool for the improvement of the agility of tracked vehicles.

In the selection of track dimensions the designer has some, although limited, freedom. It is of interest to investigate what effect the selection of the aspect ratio (length/width) of the track has on the acceleration capability of tracked vehicles under various soil conditions. The maximum tractive force that can be developed in various soils by a main track area of various aspect ratios is shown in Fig. 12 for a track area and load corresponding to that of a M60 tank. The figure shows that the effect of aspect ratio on the maximum tractive force that can be developed is minimal. It is noted that the maximum tractive force is less than that computed from the formula

$$T = cA + W.\tan\phi \tag{8}$$

where A = ground contact area

W = track load

c = cohesion

ϕ = friction angle

proposed by some authors. Figure 13 shows the maximum tractive force as the percentage of that computed by Eq. (8). The maximum tractive force, as defined by Eq. (8) is a hypothetical one, since the decrease of the bearing capacity with the increase of the tractive force prevents its full development.

The effect of approach angle on the soil resistance acting on the inclined portion (ramp) of the track can also be analyzed by the model. For example, Fig. 14 shows the variation of the horizontal and vertical component of the passive resistance encountered by the front of the track at the time the maximum soil thrust is developed. The dimensions of the track are those of the M60 tank; the soil is cohesionless sand ($\phi = 35°$). The trim has been assumed as 5 percent. The figure shows that at an approach

angle of about 30 degrees the horizontal component is nearly zero, indicating that at the time the maximum soil thrust is developed, the passive resistance at the ramp, if inclined at 30° or less, is negligible and does not add to the motion resistance.

It is also of interest to analyze the components of the resistances that oppose motion. It is noted that in the model only soil resistances are computed, mechanical resistances should be accounted for separately. The two main components of the soil resistance are the passive resistance acting on the ramp and the tangential component of track load due to the trimmed position. Typical values of these resistance components in cohesionless sand (ϕ = 35°) are shown for an assumed trim angle of three degrees in the following tabulation.

Vehicle	M60	M113
Main Track Area (ft)	13.2 x 2.32	8.75 x 1.25
Average Ground Pr. (psi)	11.8	7.6
Approach Angle	45°	30°
Horizontal Resistance on Ramp (lb)	1020	15
Horizontal Component due to Trim (lb)	2660	575
Drawbar Pull (lb)	26800	5880
Front Sinkage (ft)	.5	.20
Rear Sinkage (ft)	1.16	0.63

As it can be seen the major portion of the motion resistance consists of that due to the trimmed position of the vehicle. At times of acceleration there is a load transfer toward the rear that tends to increase the trim angle. To improve acceleration performance it is essential to counterbalance this tendency and reduce the trim angle. Design concepts that serve this purpose are presented in Section 7.

The location of the center of gravity also affects acceleration performance. The effect of the variation of the CG location in the longitudinal direction on acceleration performance is less definite. Results of an analysis performed by the rigid track-soil interaction model for two typical soil conditions are shown in Figs. 15 and 16. In the lower part of Fig 15 the variation of the ratio of the maximum soil thrust

to weight with the CG distance from the rear end of the ground contact area is shown for a cohesive soil (c = 200 pounds/square foot, ϕ = 10°) and for the M60 and XM1 track dimensions. In the upper half the respective trim angles are shown. While under these conditions a CG location more forward then the actual one would improve the acceleration performance, it would also reduce the trim angle. Since a negative trim angle means an undesirable nose down position, it limits the range of acceptable CG locations. Within this limit the possible improvement in acceleration performance by locating the CG more forward is minimal. Figure 16 shows the results of the same type of analysis for a cohesionless soil. In this case a more forward location of the CG would improve the acceleration performance appreciably without the trim angle becoming negative.

These two examples show that the type of soil strongly influences the interrelationship among acceleration performance, trim angle, and CG location. As long as commonality of the combat and support vehicles is required, there is little room for the improvement of acceleration performance via optimization of the CG location. Should, however, a tracked vehicle be designed for a specific geographical area, such as the Mideast where cohesionless soils are predominant, the location of the CG of the vehicle becomes an important design variable that affects the acceleration performance appreciably.

If power train data are available, the model can be used to predict the acceleration that the vehicle is capable of when traveling at various speeds. Figure 17 shows the predicted acceleration in cohesive soils (CI varying from 30 to 75) for the HIMAG vehicle (5 roadwheel, 45,000 pound track load configuration) and 1500 horsepower powertrain (93 percent efficiency, 250 fan horsepower). For the calculations a constant mass factor of 1.5 was assumed. Note that mechanical rolling resistance has not been included in the calculations. The horizontal, constant portion of the curves indicates the region where soil conditions control the acceleration.

The acceleration performance of various vehicles has also been analyzed by using the tentative track-soil interaction model. Figure 18 shows the results of an analysis of the effect of a hypothetical

variation of the pitch of the HIMAG vehicle. The soil is a cohesive soil, CI = 40; all other conditions are the same as in Fig. 17. Note that the predicted acceleration decreases with the decrease of pitch. Also, note that as expected, the acceleration predicted by the semirigid model is less than that predicted by the rigid model. The rigid track-soil interaction model may be thought of as the model of a track where the pitch equals the length of the ground contact area.

Figure 19 shows the results of a similar analysis for the M113 vehicle.

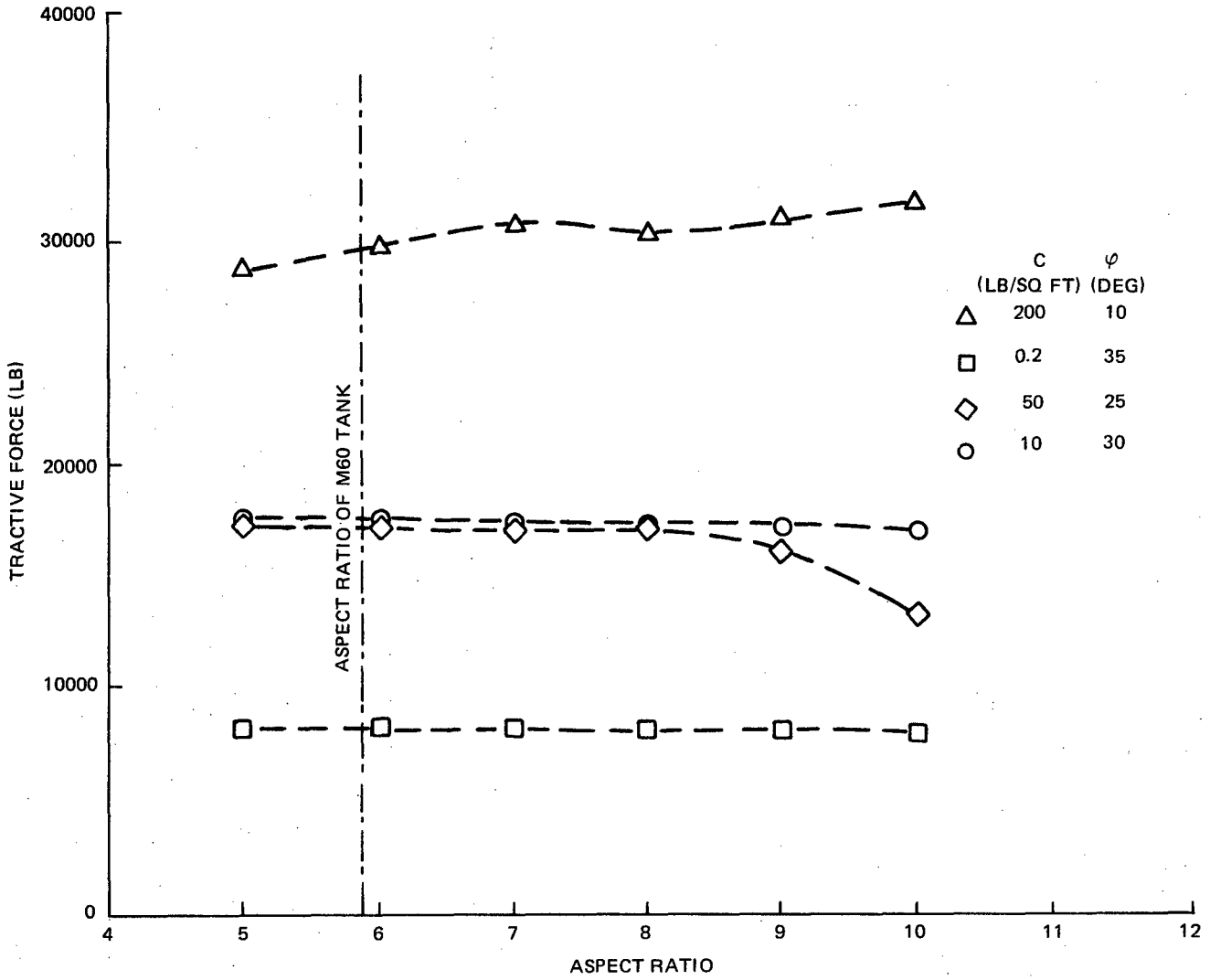

Fig. 12 Maximum Tractive Force That Main Track Area Can Develop at Various Aspect Ratios (L/B) in Various Soils. Main track area and load corresponds to that of an M60 tank

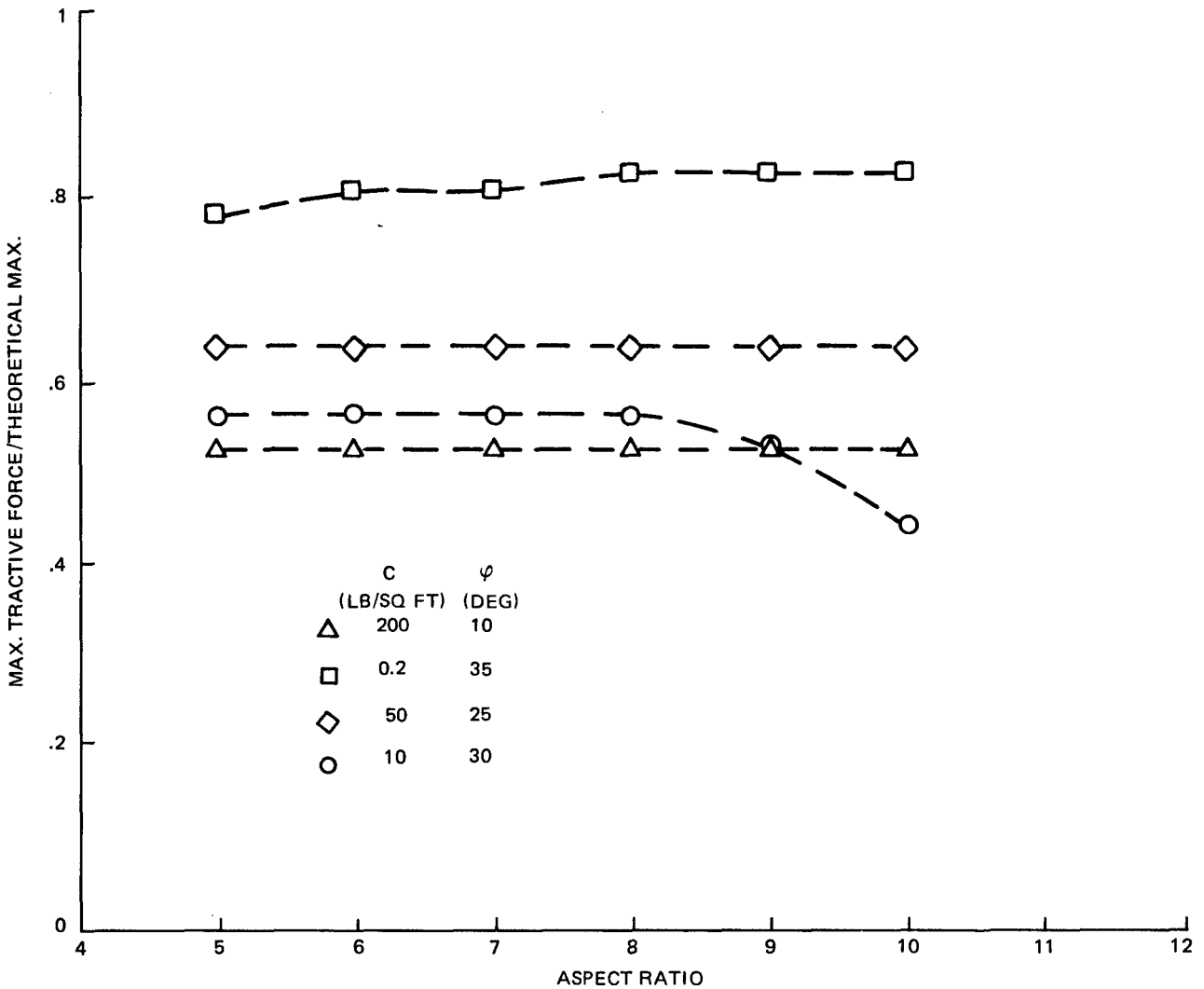

Fig. 13 Ratio of Maximum Tractive Force to Theoretical Maximum

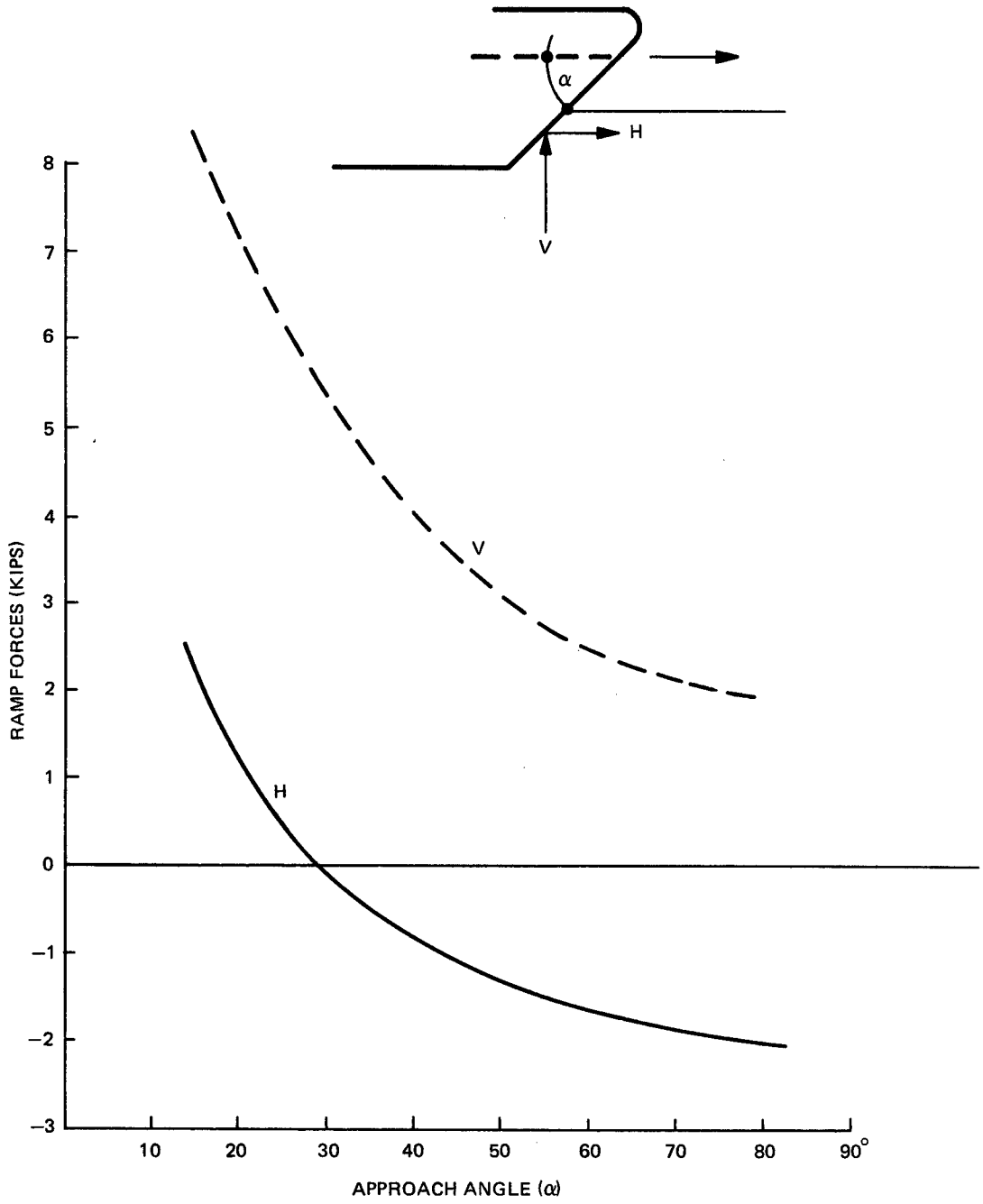

Fig. 14 The Effect of Approach Angle on the Earth Resistance Acting on the Ramp

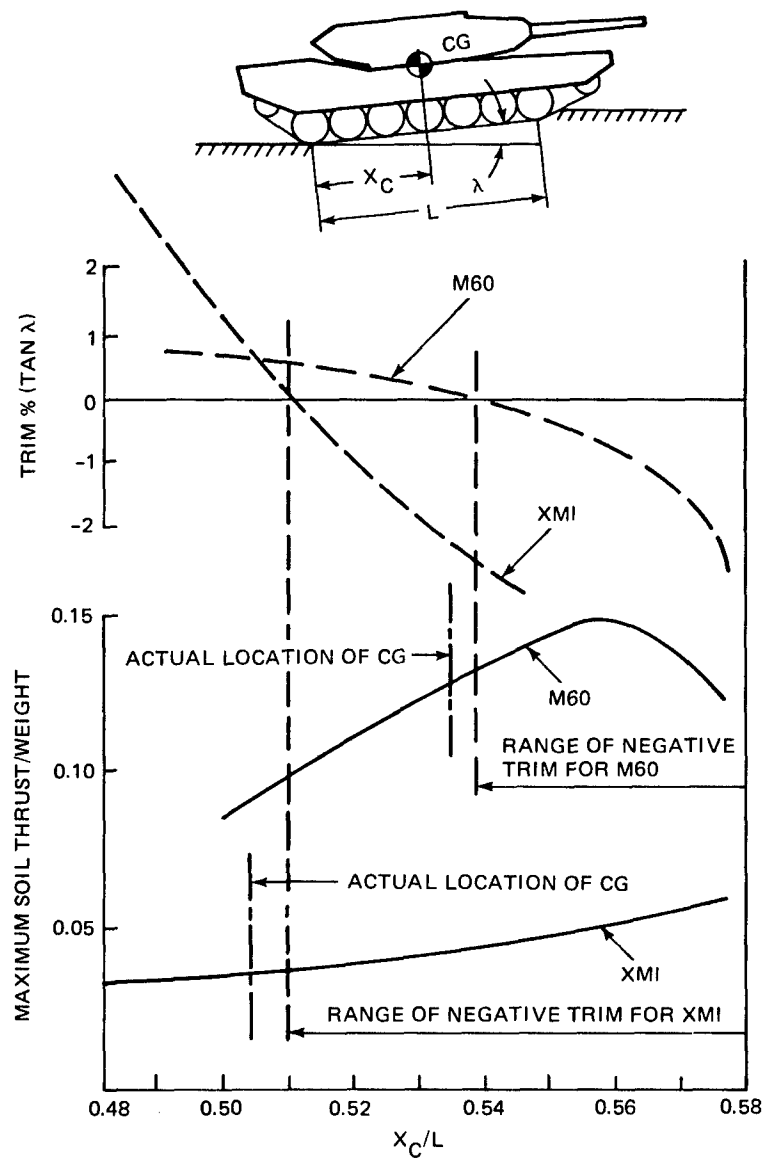

Fig. 15 Effect of the Location of CG on the Maximum Soil Thrust and Trim Angle in Cohesive Soil

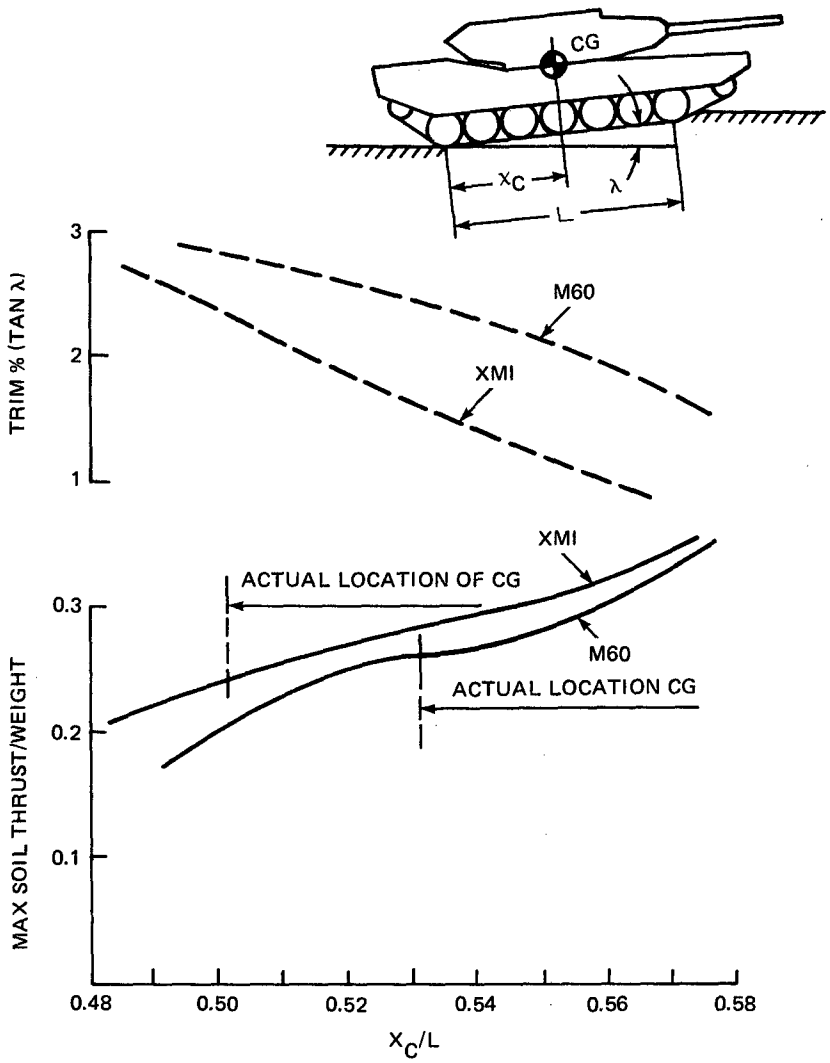

Fig. 16 Effect of the Location of CG on the Maximum Soil Thrust and Trim Angle in Cohesionless Soil

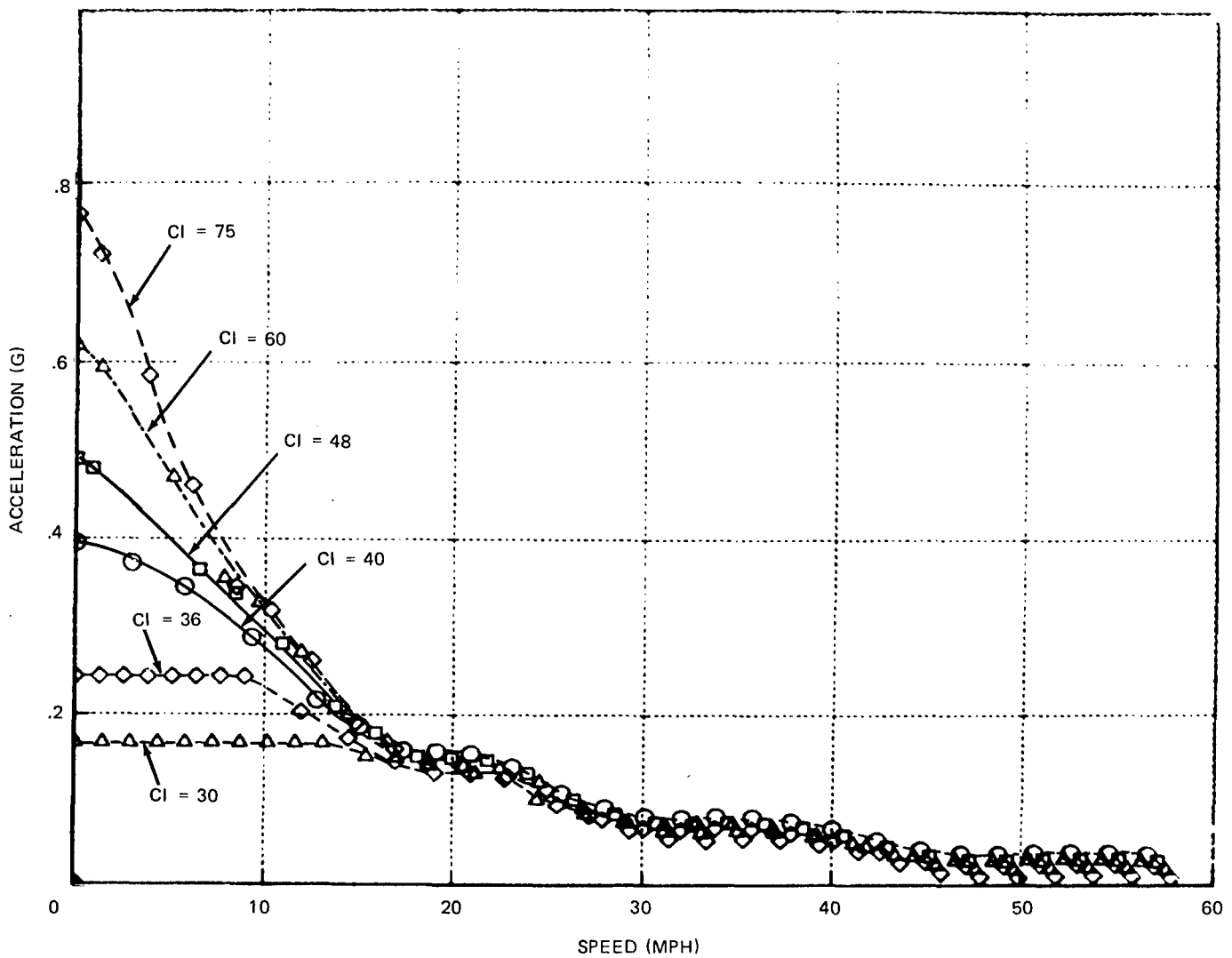

Fig. 17 Predicted Acceleration Capability of the HIMAG Vehicle in Cohesive Soils at Various Speeds. CI = cone index. 5 roadwheel – 45,000 lb configuration. Powertrain: 1500 hp, 93% efficiency fan: 205 hp

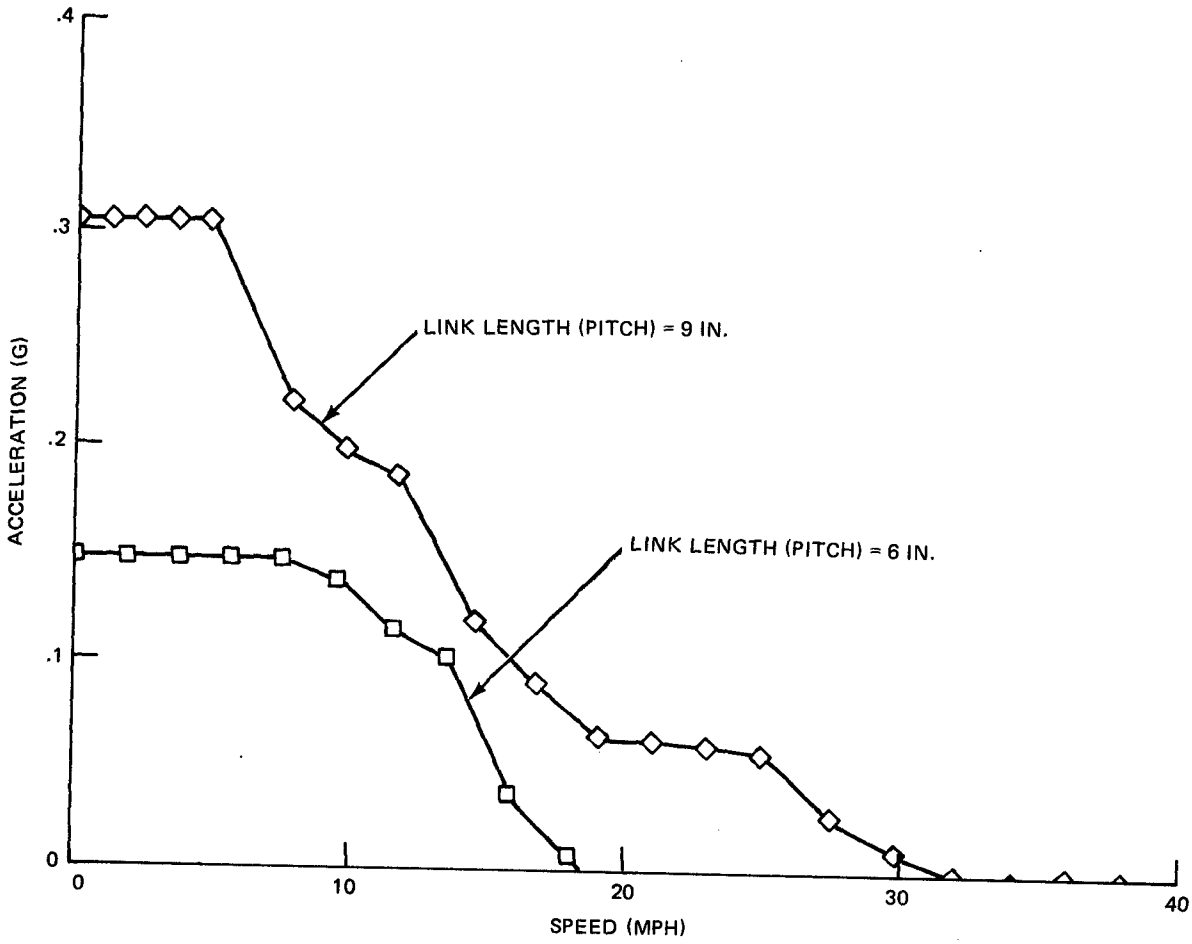

Fig. 18 Effect of Link Length (Pitch) on Acceleration. HIMAG Vehicle, 4500 lb Trackload, Five Roadwheel Configuration. Power 1500 hp, 93% efficiency; cohesive soil, CI = 40

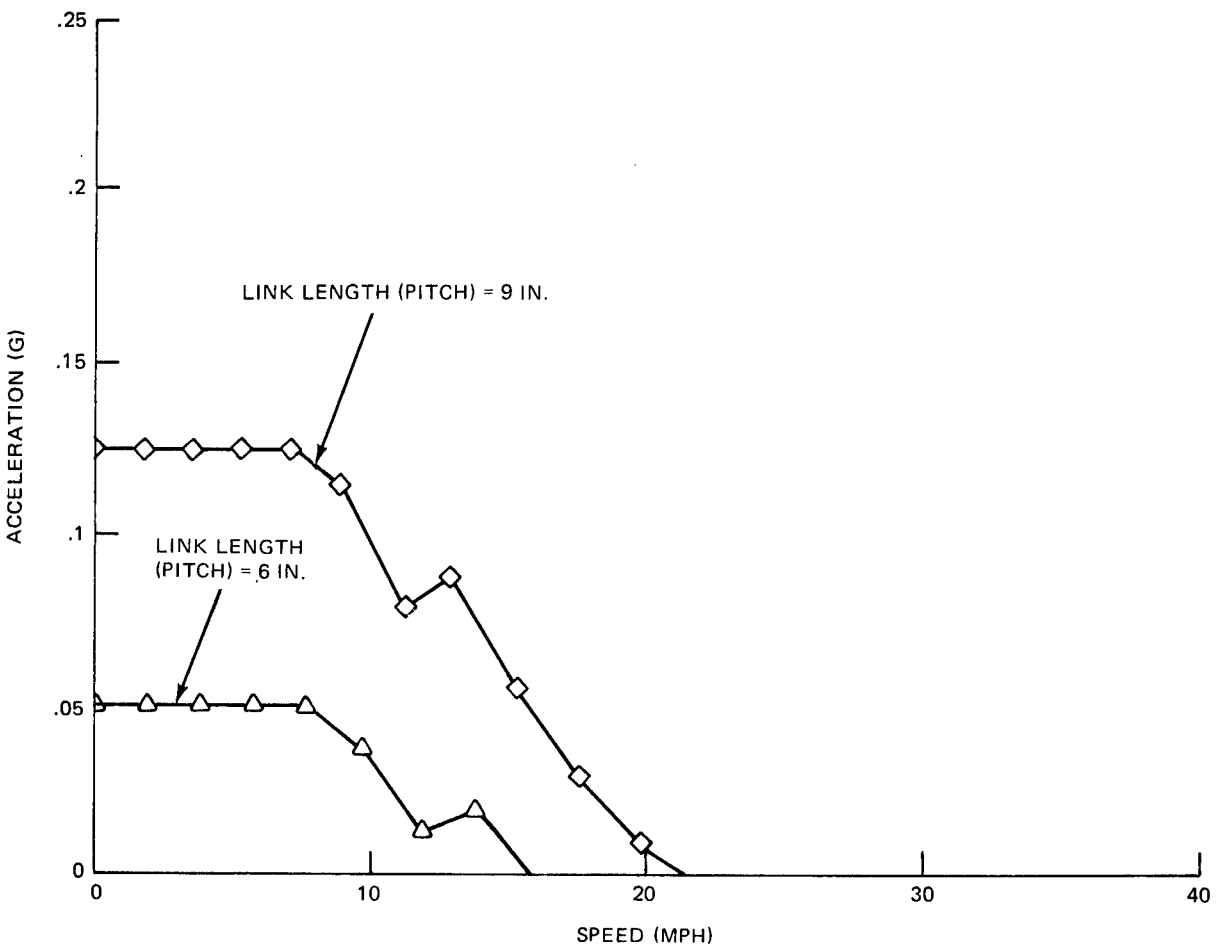

Fig. 19 Effect of Pitch Variation on Acceleration Performance Vehicle, M113 Cohesive Soil, CI = 20

6. TURNING RESISTANCES

The turning of skid steered tracked vehicles is resisted by frictional forces developed at the track-soil interface and by passive earth resistances acting at the side faces of the track. For the improvement of the maneuverability of tracked combat vehicles it is essential that these turning resistances be minimized and their interrelationship with the characteristics of the turning maneuver (turning radius, speed), track performance, and soil properties be established. These interrelationships are discussed in this section.

LATERAL SHEAR RESISTANCES AT THE TRACK-SOIL INTERFACE

The shear resistances that oppose the lateral movement of track are commonly characterized by a coefficient of friction, μ_y, that may not be the same as μ_x, opposing forward motion (Refs. 4-6). The lateral shear resistance is computed as

$$\tau_y = \mu_y p \tag{9}$$

where p = normal pressure.

This formula is untenable since it does not conform with the following experimentally validated characteristics of shear resistance development:

a) The shear resistance is of the Coulombic form; that is, it consists of two components, one being independent of the normal pressure. Thus, Eq. (9) is limited to purely frictional soil

b) The shear resistance develops gradually with the relative displacement of the sliding bodies. Equation (9) implies that the ultimate shear resistance, τ_y, is always developed, regardless of the relative displacement of track and soil

A fundamental characteristic of frictional shear resistance is that it acts in the direction opposite to the motion. In the case of a turning track, the direction of motion is determined by the instantaneous velocity vector (Fig. 20). Thus the shear stress representing the frictional resistance developed at a point of the track-soil interface is a vector, opposite and colinear with the instantaneous velocity vector, v_i. In the case of straight line motion the magnitude of the shear stress vector can be

conveniently determined from the Janosi-Hanamoto equation that relates shear stress to slip. Unfortunately, the concept of slip cannot be directly applied to the case of turning since the definition of slip is based on colinear velocities while in the case of turning the actual and theoretical velocities diverge. In this respect it is also useful to consider that shear stresses cause slip and not vice versa. Thus, the correct formulation of the problem of slip for a turning vehicle is as follows.

> At a point of the track-soil interface of a turning vehicle a shear stress τ is generated that is colinear with and opposite to the direction of the instantaneous velocity vector, v_i. The longitudinal component of this shear stress is τ_x. One should then determine the magnitude of slip that is associated with the generation of a shear stress equal to τ_x in straight line motion.

This formulation allows straightforward calculation of slip in the conventional sense and also allows the determination of the τ_y component of the shear stress that resists the turning of the track. In problem solutions, of course, an inverse procedure may be applied and the τ_x component of the shear stress may be calculated for a given slip.

Qualitatively, the lateral shear resistance determined as the lateral component, τ_y, of the shear stress in the direction of the instantaneous velocity vector (τ) meets the criteria listed under a and b if the longitudinal component of the interface shear stress, τ_x, is determined on the concept of interface friction angle, (Fig. 21). If the mobilized shear stress is expressed as a function of the interface friction angle, δ, then

$$\tau_x = \tau_{mob} = (\sigma_n + \psi) \tan \delta \qquad (10)$$

where σ_n = normal stress

ψ = c.cot ϕ (c=cohesion, ϕ = friction angle)

δ = angle of interface friction

The maximum value of the interface friction angle, δ, is the friction angle of soil, ϕ.

$$\tau_{max} = (\sigma_n + \psi) \tan \delta_{max} = (\sigma_n + \psi) \tan \phi = c + \sigma_n \tan \phi \qquad (11)$$

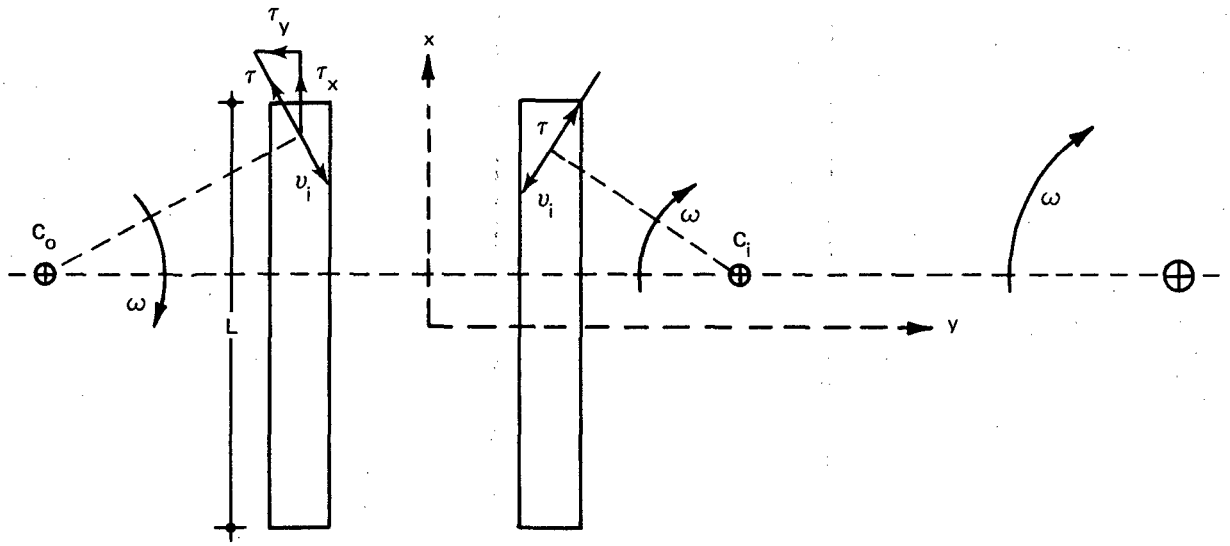

Fig. 20 Instantaneous Velocity and Shear Stress Generated by a Turning Tracked Vehicle

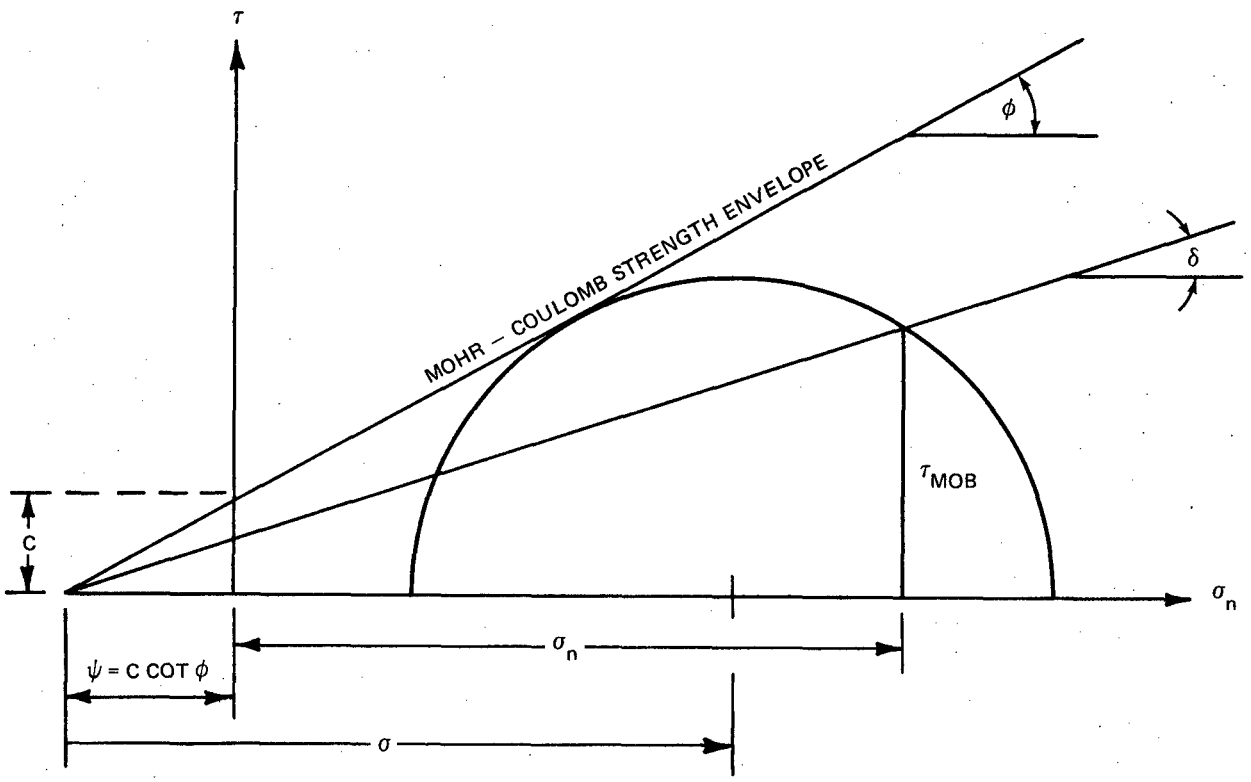

Fig. 21 Mohr Circle, Mobilized Shear Stress and Interface Friction Angle

The mobilized shear stress can be expressed in a form similar to that of the Janosi-Hanamoto equation,

$$\tau_{mob} = \tau_{max} (1 - e^{-s/k}) \tag{12}$$

where s = slip

k = slip parameter

Combination of these equtions yields

$$\tan \delta = \tan \delta_{max} (1 - e^{-s/k}) \tag{13}$$

The slip is defined as follows

$$s = (1 - \frac{V_a}{V_{th}}) \tag{14}$$

where s = slip

V_a = actual velocity of vehicle at track centerline

V_{th} = theoretical velocity

$|V_{th}| = |V_t|$ = track velocity

The maximum value of slip is 1, or 100 percent at which the vehicle comes to stop no matter what the applied track velocity is. The slip equation may also be expressed in terms of slip velocity, as follows.

$$s = \frac{V_{th} - V_a}{V_{th}} = \frac{V_s}{V_{th}} \tag{15}$$

where V_s = slip velocity.

In applying the above definition of slip to the motion of the inner track in turning, the slip becomes negative (since $V_a > V_{th}$) and may exceed 100 percent. To have the range of slip consistent for the outer and inner track it is convenient to define the slip for the inner track as follows:

$$s = \frac{|V_s|}{|V_{max}|} \tag{16}$$

where $V_{max} = \max (V_{th}, V_a)$

The above definition of slip makes it possible to use the same shear stress-slip relationship for both the outer and inner track. For example, Eq. (12) would read

$$\tau_{mob} = \text{sign} \frac{V_s}{V_{max}} \cdot \tau_{max} (1 - e^{-s/k}) \quad (17)$$

allowing for the fact that τ is always opposite the slip velocity. The maximum shear stress, τ_{max}, may be expressed by a Coulomb type equation as

$$\tau_{max} = c + \sigma_n \tan \phi \quad (18)$$

While the above shear-slip relation is formally the same for the outer and inner track, the magnitude of the slip necessary to develop a given shear stress will generally be different for the outer and inner track for the following reasons: "Slip" consists of two components, slip due to soil deformation (also called "contact slip") and slip due to differential displacement between soil and track. However, in the case of the inner track, horizontal soil deformation is in the direction of travel; it therefore reduces the slip of the inner track. Thus, the "k" value in Eq. (12) will be generally lower for the inner than for the outer track.

DETERMINATION OF LATERAL FORCES ACTING ON THE SIDE FACE OF TRACKS DURING TURNING

The turning of tracked vehicles is resisted by frictional forces at the track-soil interface and, in addition, by lateral forces resisting the cutting action of the side faces of the track. These forces are generated wherever the paths of the various points along the side of the track cross an area that has not been previously compacted by the track. The lateral forces generated in these areas are shown in Fig. 22.

The lateral forces opposing the motion of the track in a curved path can be resolved into components normal and tangential to the side of the track. The tangential component is part of the motion resistance. The normal component depends on the passive pressure exerted by the earth against the track forcing itself sideways into the wall of the rut that was formed by the forward movement of the track (Fig. 23). The passive earth pressure depends on the strength properties of soil and the geometric configuration of the rut wall and track and can be determined by plasticity theory methods. In the case of a cohesive soil the wall of the rut stands vertically. At a relatively low sinkage the side face of the track, pushed by lateral movement against the wall of the rut, creates a slip line field

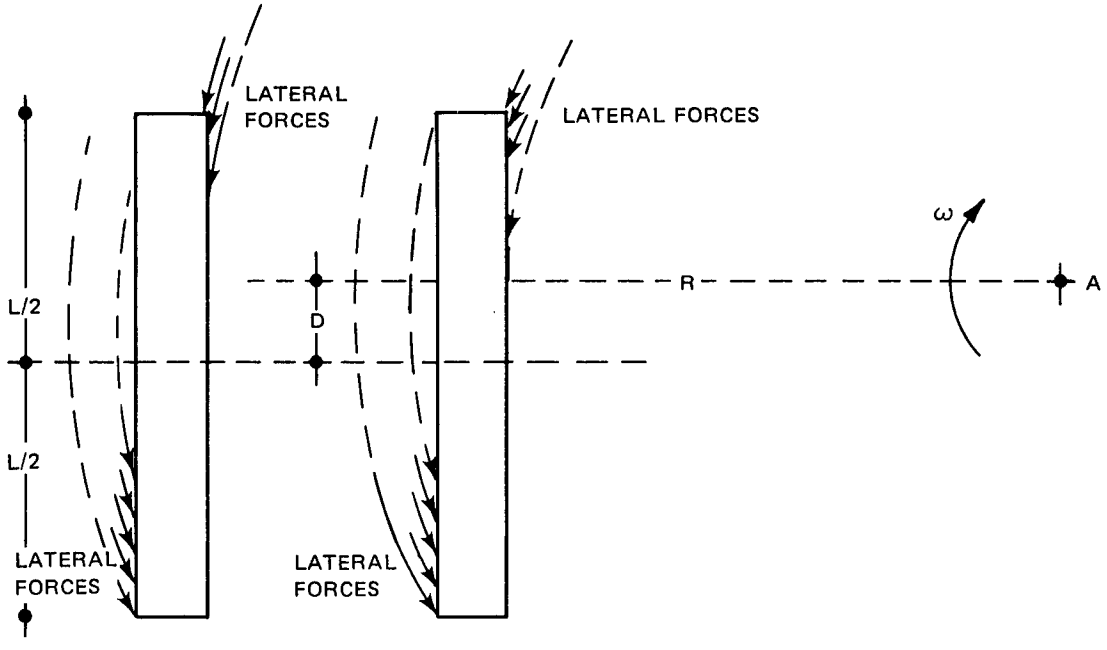

Fig. 22 Lateral Forces Generated at the Side Forces of the Track in Turns

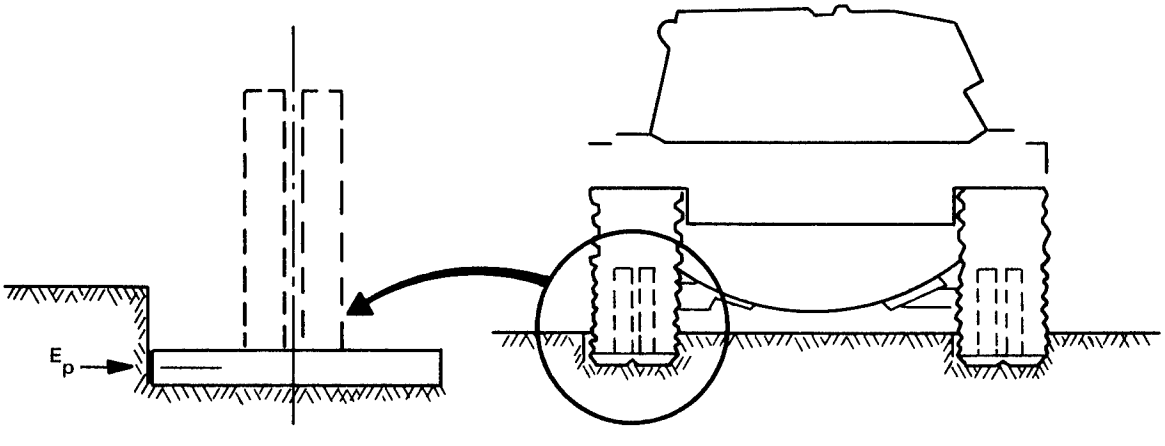

Fig. 23 Passive Earth Pressure (E_p) Resists Lateral Track Movement

as shown in Fig. 24. In cohesionless soils the vertical walls of the rut slump down and come to rest at the angle of repose. Figure 25 shows the slip line fields for this case. In cohesive soils and high sinkage the slip line field may not reach the original surface but bends back to the vertical face of the rut, as shown in Fig. 26. In this case the soil above the slip lines is undercut and would slump down as that soil mass loses its support.

As can be seen from Figs. 24 through 26, it is always possible to construct a slip line field for the determination of the passive earth pressure. However, because the pattern of the slip line fields changes with the geometry of the boundary conditions it is difficult to prepare a general solution that would be usable for all conceivable variations of the geometric boundary conditions. Detailed studies showed, however, that even though the slip line patterns vary appreciably with the geometry of the boundary conditions the average passive pressure that develops in cohesive soil can be closely approximated by the following formula

$$q = c \cot \phi \left[\frac{e^{\pi \tan \phi}}{\cos^2 \phi} - 1 \right] \tag{19}$$

where q = average passive pressure

c = cohesion

ϕ = friction angle.

Figure 27 shows the values of the passive pressure, or lateral cutting resistance for various cone indices, using the approximate relationship between strength properties and cone index developed for Buckshot clay.

In cohesive soils the lateral cutting resistance may amount to 25-30 percent of the lateral frictional resistance which develops in turns. In cohesionless soils the lateral cutting resistance amounts to only 1 to 2 percent of the lateral frictional resistance and, therefore, may be neglected in turning resistance calculations.

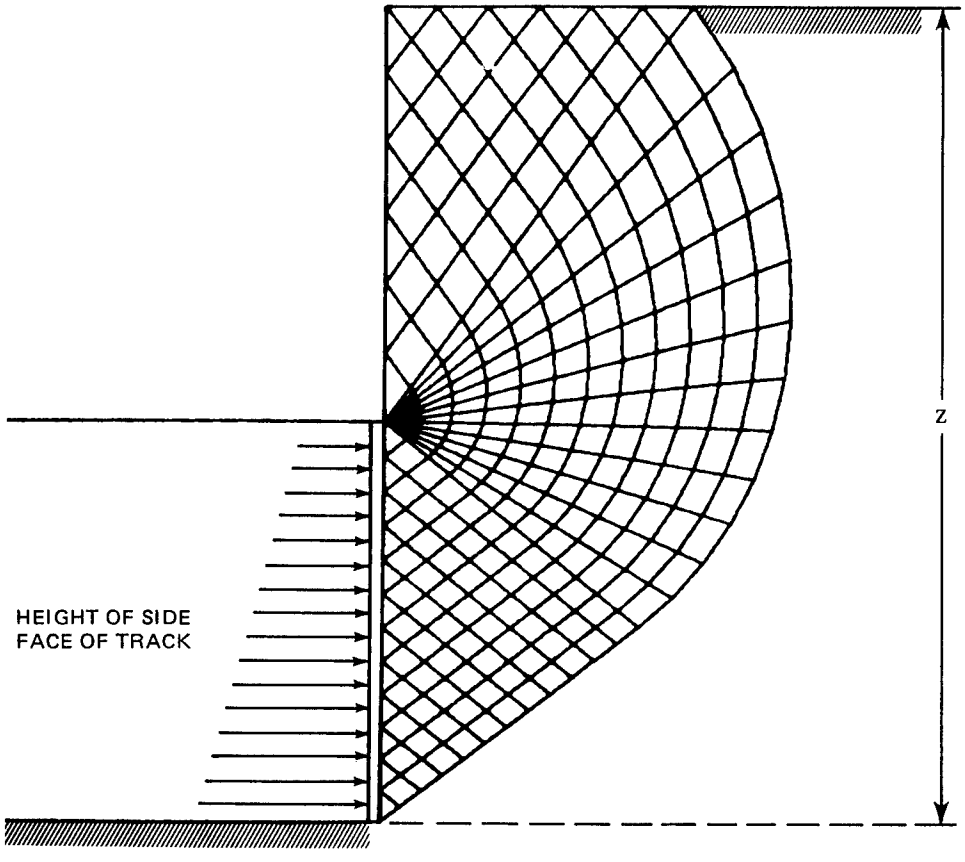

Fig. 24 Slipline Field for the Determination of Passive Earth Pressure in the Case of Cohesive Soil and Small Sinkage (Z)

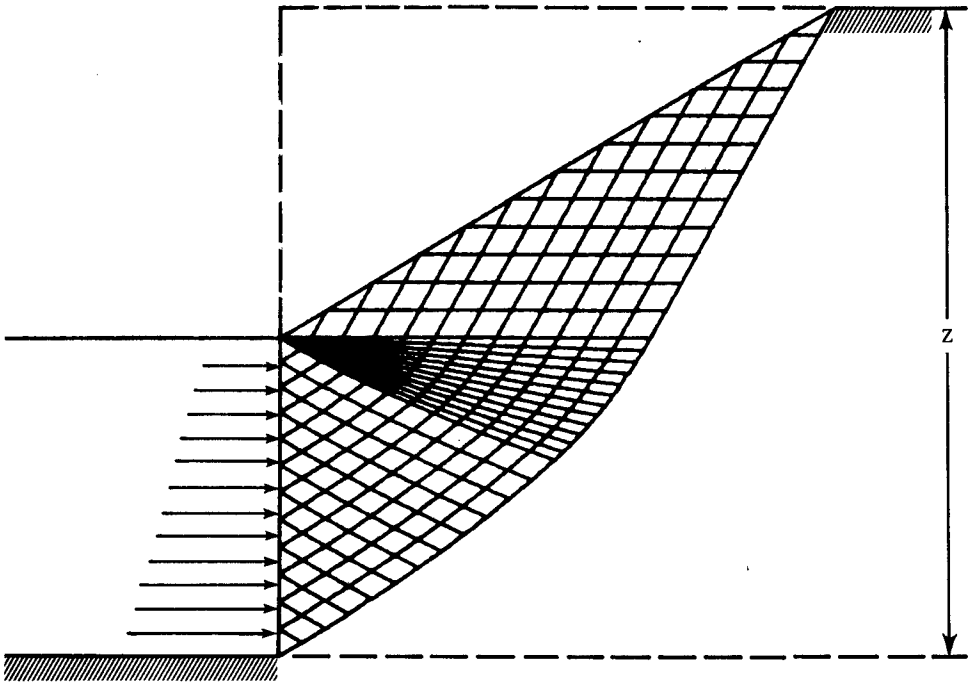

Fig. 25 Slipline Field for the Determination of Passive Earth Pressure in the Case of Cohesionless Soil

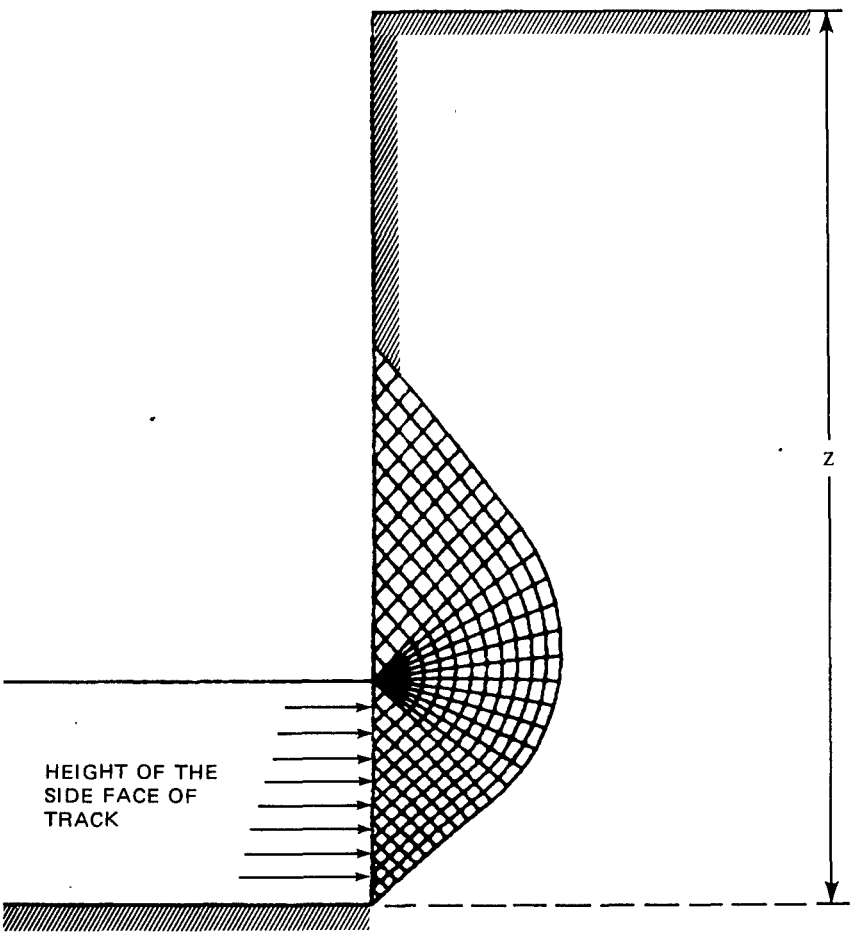

Fig. 26 Slipline Field Undercuts the Wall of the Rut in Cohesive Soil and Large Sinkage (Z)

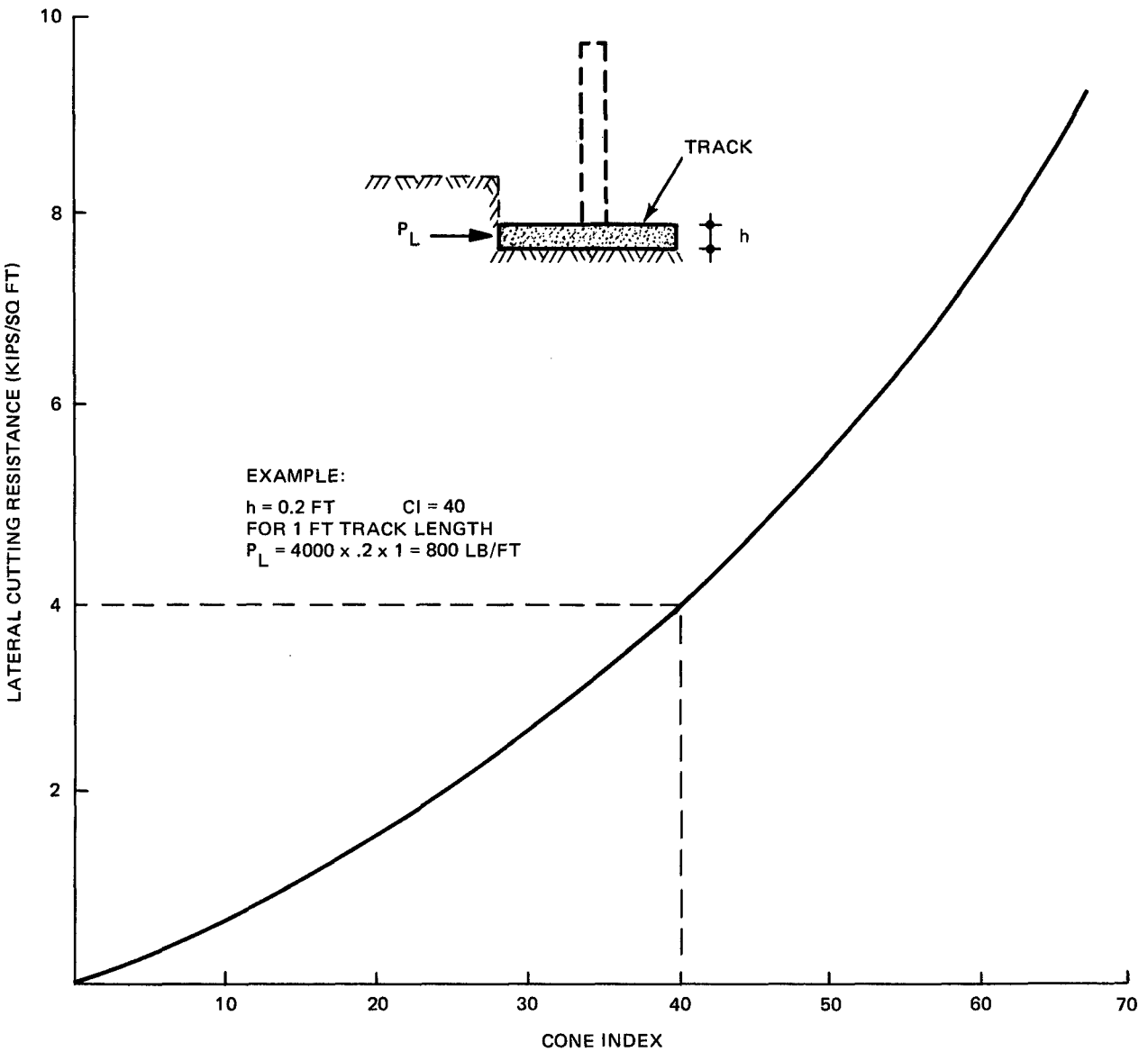

Fig. 27 Lateral Cutting Resistance for Various Cone Index Values

7. CONCEPTS PROPOSED FOR THE IMPROVEMENT OF THE AGILITY OF TRACKED VEHICLES

Improvement of the agility of tracked vehicles requires the improvement of their acceleration capability. This capability may be limited by engine power or by soil conditions that limit the development of soil thrust. The accelerating capability of vehicles that have high nominal ground pressure and high engine power (i.e., most modern combat vehicles) is more likely to be limited by soil conditions than that of lighter and less powerful vehicles.

Analysis of the accelerating capability of tracked vehicles by means of both the rigid and semirigid track-soil interaction model conclusively show that during acceleration the soil conditions beneath the last roadwheel are critical. For the improvement of accelerating capability it is essential that the critical situation at the last roadwheel be alleviated. Design concepts that address this problem are presented in the following subsections.

UNEQUAL SPACING OF ROADWHEELS

Traditionally, the roadwheels of the tracked combat and support vehicles of the Army are equally spaced. At constant low speed the load on equally spaced roadwheels is approximately the same. However, during acceleration, load transfer changes the load distribution on the roadwheels, the last roadwheel carrying the heaviest load. An unequal spacing, such as shown schematically in Fig. 28 reduces the load on those roadwheels more closely spaced in the rear and increases the load on the spread out front roadwheels. The critical condition beneath the last roadwheel is alleviated by the reduction of the load; the trim angle is reduced; and the acceleration performance is improved.

OVERLAPPING ROADWHEEL IN THE REAR

A row of overlapping roadwheels has been applied in various tank designs to insure a more uniform distribution of the ground pressure. While such double rows of roadwheels are advantageous from the viewpoint of track-soil interaction, they restrict the obstacle crossing performance of the vehicle. Using only one overlapping roadwheel in the rear (Fig. 29) improves acceleration performance without harming obstacle crossing performance.

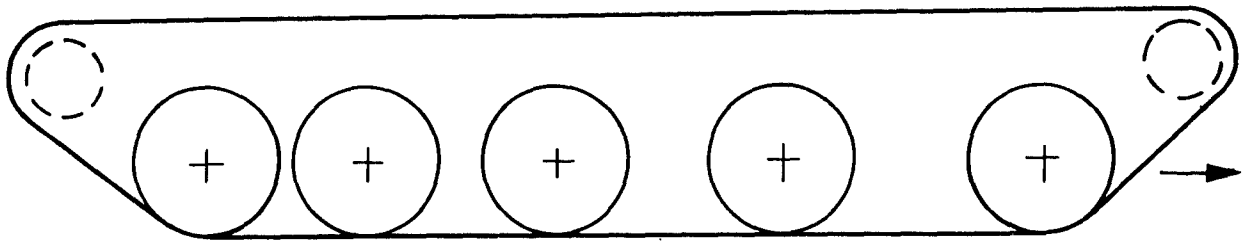

Fig. 28 Schematic Arrangement of Unequally Spaced Roadwheels

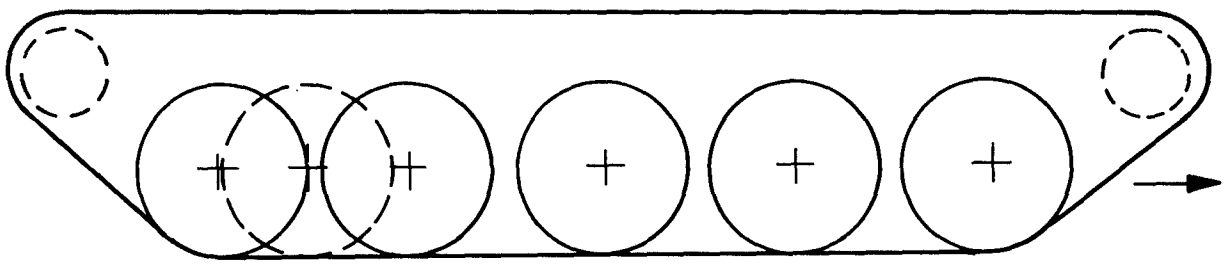

Fig. 29 Schematic Arrangement of an Overlapping Roadwheel Between the Last Two Roadwheels

USE OF SEMIGIRDERIZED TRACKS

The analyses by the semirigid track soil interaction model presented in Section 5 clearly show the advantages of a hypothetical increase in the pitch (length of the links) in a pin-jointed track. In practice, performance considerations are overruled by other requirements in the selection of pitch and limit the range within which the pitch could be increased without serious drawbacks. A concept of track design having the advantages of a longer pitch in its interaction with soil but which would otherwise act as one with a shorter pitch is shown in Fig. 30. This track is a transition between girderized and pin-jointed tracks and uses girders to stiffen pairs of links but retains pin joints between the pairs of links, and, therefore, it may be called "semigirderized" track. Such a track design would allow greater flexibility in selecting the pitch and at the same time offer the advantages of having the effective bearing area of the track increased.

ADAPTIVE SUSPENSION SYSTEM

The analyses presented in Section 5 show that the location of CG of tracked vehicles relative to the center of the main ground contact area affects acceleration performance, and that for a specific soil condition there is an optimum CG location for best acceleration performance. From the viewpoint of track-soil interaction, a variable CG location would be desirable. An adaptive suspension system that would allow the engagement and disengagement of the first and last roadwheel whenever soil and acceleration conditions require is shown schematically in Fig. 31. With such a system the CG location relative to the main ground contact area could be adapted to the momentary conditions for optimum acceleration performance.

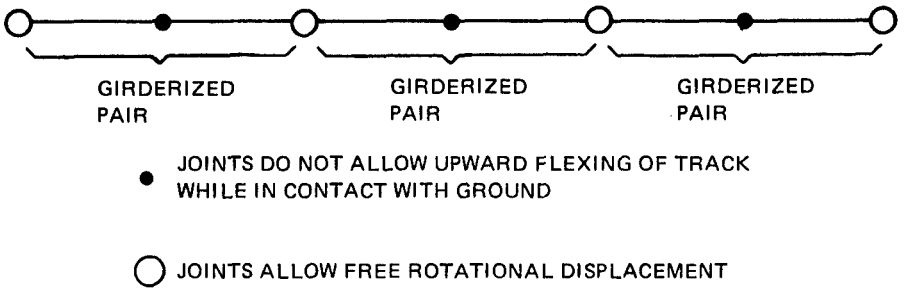

Fig. 30 Scheme of Semigirderized Track

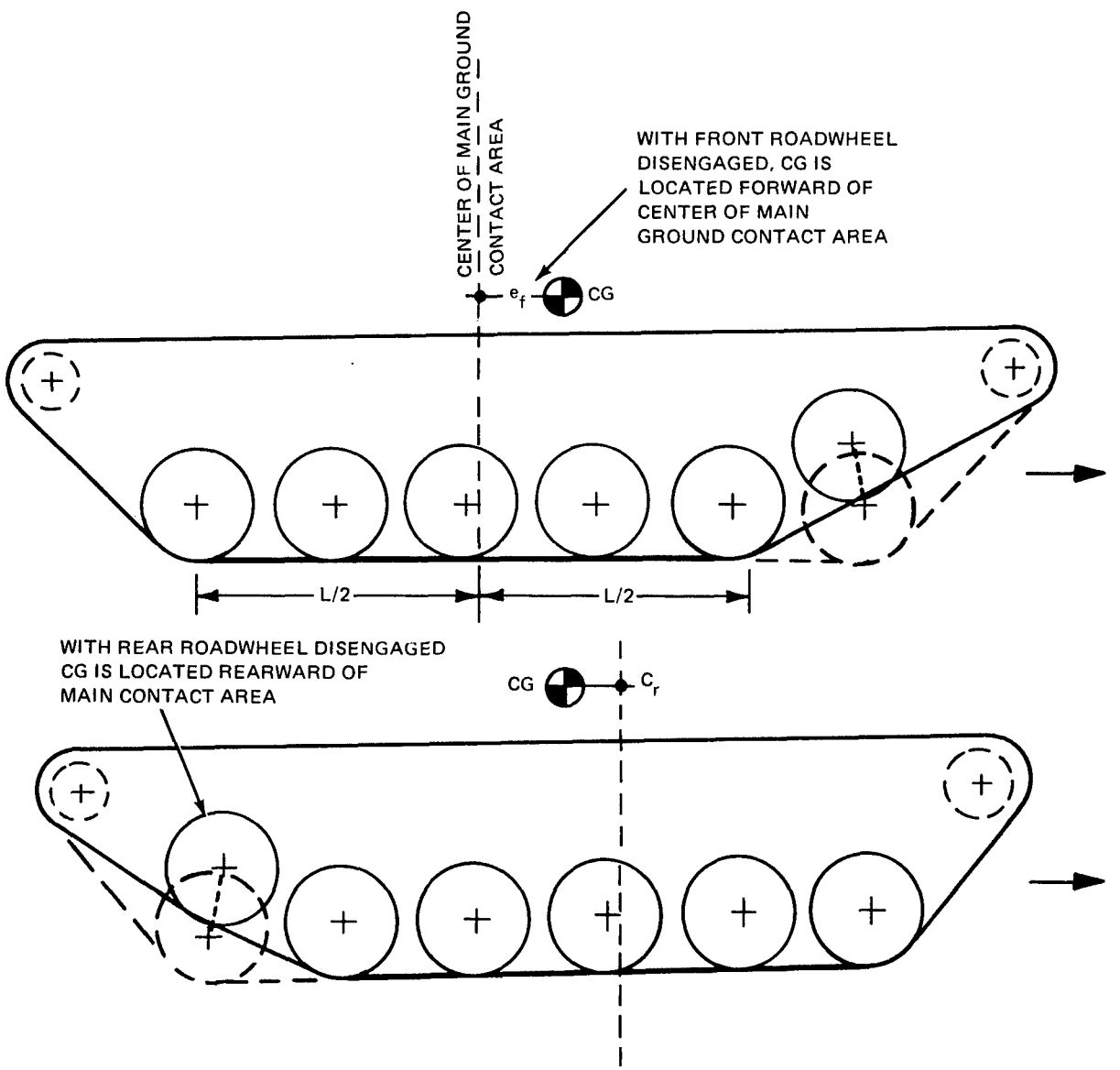

Fig. 31 Schematics of Adaptive Suspension System

8. CONCLUSIONS AND RECOMMENDATIONS

A rigid track-soil interaction model has been developed for the determination of maximum soil thrust and acceleration perforamnce. Analyses performed by means of the model show that the effect of track length/width ratio on acceleration performance is minimal. The location of CG affects the acceleration performance differently in the various types of soils. Significant improvement in acceleration performance by optimizing the CG location could be achieved only if specific vehicles were to be designed for specific soil conditions prevailing in various strategically important geographical areas.

Analyses performed by the rigid track-soil interaction showed that under certain conditions the assumption of rigid track geometry results in unrealistic soil response. As an alternate, a semirigid track-soil interaction model has been developed. Preliminary analyses performed using this model show that acceleration performance is governed by the interaction between the track links beneath the last roadwheel and the soil supporting these links. It is recommended that a flexible track-soil interaction model with appropriate representation of the freedom of track joint displacements be developed for the detailed analysis of the effect of track flexibility on acceleration performance.

Several concepts aimed at improving acceleration performance are presented. Of these, the concepts of an additional overlapping roadwheel in the rear and semigirderized track are the most promising. It is recommended that these concepts be developed enough so that field experiments could be performed with appropriately modified vehicles to validate them.

9. REFERENCES

1. Karafiath, L.L., Nowatzki, E.A., Ehrlich, I.R., and Capin, J., "An Application of Plasticity Theory to the Solution of the Rigid Wheel-Soil Interaction Problem," U.S. Army Tank Automotive Command Mobility Systems Laboratory Technical Report No. 11758(LL141), March 1973.

2. Karafiath, L.L., "Development of Mathematical Model for Pneumatic Tire-Soil Interaction," U.S. Army Tank Automotive Command Mobility Systems Laboratory Tech. Report No. 11900(LL147), July 1974.

3. Karafiath, L.L. and Sobierajski, F.S., "Effect of Speed on Tire-Soil Interaction and Development of Towed Pneumatic Tire-Soil Model," U.S. Army Tank Automotive Command Mobility Systems Laboratory Tech. Report No. 11997(LL151), October 1974.

4. Seeds, W. "Tracked Vehicles - An Analysis of the Factors Involved in Steering," Automobile Engineer, April 1950.

5. Kitano, M. and Jyozaki, H., "A Theoretical Analysis of Steerability of Tracked Vehicles," Journal of Terramechanics, Vol. 13, No. 4, 1976.

6. Smith, M.D., "Investigation of Tracklaying Vehicle Steer Requirements," Final Engineering Report, OTAC Research and Development Division, AD 486102, June 1958.

DISTRIBUTION LIST
(As of 1 June 1978)

Please notify USATARADCOM, DRDTA-ZSA, Warren, Michigan 48090, of corrections and/or changes in address.

No. of Copies

50 Commander
US Army Tank Automotive Research and Development Command
Warren, MI 48090

2 Hqs, DA
Ofc of Dep Chief for Rsch, Dev & Acquisition
ATTN: DAMA-WSW
LTC Bertel R. Bertils
Washington, D.C. 20310

1 Superintendent
US Military Academy
ATTN: Dept of Engineering
Course Director for Automotive Engineering
West Point, NY 10996

1 Commander
US Army Logistic Center
ATTN: ATCL-CC
Mr. J. McClure
Ft. Lee, VA 23801

2 US Army Research Office
P.O. Box 12211
ATTN: Mr. James Murray, Dr. Mayer
Research Triangle Park, NC 27709

1 Hq, DA
ATTN: DAMA-ARZ-D
Dr. Herschner
Washington, D.C. 20310

1 Hq, DA
Ofc of Dep Chief of Staff for Rsch, Dev & Acquisition
Attn: DAMA-REZ-E
Dr. Charles Church
Washington, D.C. 20310

1 Mr. H.C. Hodges
Nevada Automotive Test Center
Box 234
Carson City, NV 89701

1 Mr. W.S. Hodges
Lockheed Missile & Space Corporation
Ground Vehicle Systems
Department 50-24, Bldg. 528
Sunnyvale, CA 94088

1 Mr. R.D. Wismer
Deere & Company
Engineering Research
3300 River Drive
Moline, IL 61265

1 Oregon State University
Library
Corvallis, Oregon 97331

1 Southwest Research Institute
ATTN: Mr. R.C. Hemion
8500 Culebra Road
San Antonio, TX 78228

1 FMC Corporation
Technical Library
P.O. Box 1201
San Jose, CA 95108

1 Mr. J. Appelblatt
Director of Engineering
Cadillac Gauge Co.
P.O. Box 1027
Warren, MI 48090

2 Chrysler Corporation
Mobility Research Laboratory,
Defense Engineering
Attn: Dr. B. Van Duesen, Mr. J. Cohron
Department 6100
P.O. Box 751
Detroit, MI 48231

1 Library
CALSPAN Corporation
Box 235
4455 Genesse Street
Buffalo, NY 14221

1 Commander
US Army Concept Analysis Agency
Long Range Studies
8120 Woodmont Avenue
Bethesda, MD 20014

1 Dept of the Army
Office Chief of Engineers
Chief Military Programs Team
Rsch & Dev Office
ATTN: DAEM-RDM
Washington, D.C. 20314

2 Director
US Army Corps of Engineers
Waterways Experiment Station
P.O. Box 631
Vicksburg, MS 39180

3 Director
U.S. Army Corps of Engineers
Waterways Experiment Station
Attn: Mobility & Environmental Laboratory
P.O. Box 631
Vicksburn, MS 39180

4 Director
US Army Cold Regions Research & Engineering Lab
Attn: Dr. Freitag, Dr. W. Harrison, Dr. Liston,
Library
P.O. Box 282
Hanover, NH 03755

3 President
Army Armor and Engineer Board
Attn: COL Fitzmorris, LTC Dennis, Mr. Kelton
Ft. Knox, KY 40121

1 Commander
US Army Artic Test Center
APO 409
Seattle, Washington 98733

2 Commander
US Army Test and Evaluation Command
ATTN: AMSTE-BB and AMSTE-TA
Aberdeen Proving Ground, MD 21005

2 Commander
Rock Island Arsenal
Attn: SARRI-LR
Rock Island, IL 61201

2 Commander
US Army Yuma Proving Ground
ATTN: STEYP-RPT, STEYP-TE
Yuma, Arizona 85364

1 Mr. Frank S. Mendez, P.E.
Technical Director
US Army Tropic Test Center
ATTN: STETC-TA
Box 942
Fort Clayton, Canal Zone 09827

1 Commander
US Army Natick Laboratories
ATTN: Technical Library
Natick, Massachusetts 01760

1 Director
US Army Human Engineering Laboratory
ATTN: Mr. Eckels
Aberdeen Proving Ground, MD 21005

2 Director
US Army Ballistic Research Laboratory
Aberdeen Proving Ground, MD 21005

3 Director
US Army Material Systems Analysis Agency
ATTN: AMXSY-CM, Messrs. D. Woomert, W. Niemeyer, W. Criswell
Aberdeen Proving Ground, MD 21005

12 Director
Defense Documentation Center
Cameron Station
Alexandria, VA 22314

1 US Marine Corps
Mobility & Logistics Division
Development and Ed Command
Attn: Mr. Hickson
Quantico, VA 22134

1 Mr. A. M. Wooley
West Coast Test Branch
Mobility and Support Division
Marine Corps Base
Camp Pendleton, CA 92055

1 Naval Ship Research & Dev Center
Aviation & Surface Effects Dept.
Code 161
Attn: E. O'Neal & W. Zeitfuss
Washington, D.C. 20034

1 Director
National Tillage Machinery Laboratory
Box 792
Auburn, Alabama 36830

1 Director
USDA Forest Service Equipment Dev Center
444 East Bonita Avenue
San Dimes, CA 91773

1 Director
Keweenaw Research Center
Michigan Technological University
Houghton, MI 49931

1 Engineering Societies Library
345 East 47th Street
New York, NY 10017

1 Dr. M.G. Bekker
224 East Islay Drive
Santa Barbara, CA 93101

1 Dr. I.R. Ehrlich, Dean for Research
Stevens Institute of Technology
Castle Point Station
Hoboken, NJ 07030

2 Grumman Aerospace Corporation
Attn: Dr. L. Karafiath, Mr. E. Markow
Plant 35
Bethpage, NY 11714

1 Dr. Bruce Liljedahl
Agricultural Engineering Department
Purdue University
Lafayette, IN 46207

1 Dr. W.G. Baker
Dean, College of Engineering
University of Detroit
4001 W. McNichols
Detroit, MI 48221

1 Mr. Sven E. Lind
SFM, Forsvaretsforskningsanstalt
Avd 2
Stockholm, 80, Sweden

2 Mr. Rolf Schreiber
c/o Bundesamt Fuer Wehrtechnik
Und Beschaffung - KGII 7 -
5400 Koblenz
Am Rhein 2-6 Germany

1 Foreign Science & Technology Ctr
220 7th Street North East
ATTN: AMXST-GEI
Mr. Tim Nix
Charlottesville, VA 22901

1 General Research Corporation
ATTN: Mr. A. Viilu
7655 Old Springhouse Road
Westgate Research Park
McLean, VA 22101

2 Commander
US Army Development & Readiness Command
Attn: Dr. Norm Klein, Mr. Lindwarm
5001 Eisenhower Avenue
Alexandria, VA 22333

1 Battelle
Columbus Division
Advanced Concepts Laboratory
P.O. Box 339
Warren, Michigan 48090

1 Major T. Covington
Department of the Army, Office of the Chief of Staff
DAMA-CSS
Washington, D.C. 20310

1 D. R. Haley
DARCOM - DRCDE
5001 Esienhower Avenue
Alexandria, VA 22333

1 BDM Company
P.O. Gox 2019
1340 Munras Street
Monterey, CA 93940

1 Naval Post Graduate School
Attn: D. Sam Perry
Monterey, CA 93940

UNCLASSIFIED

SECURITY CLASSIFICATION OF THIS PAGE *(When Data Entered)*

REPORT DOCUMENTATION PAGE		READ INSTRUCTIONS BEFORE COMPLETING FORM
1. REPORT NUMBER 12380	2. GOVT ACCESSION NO.	3. RECIPIENT'S CATALOG NUMBER
4. TITLE *(and Subtitle)* Track-Soil Interaction Model for the Determination of Maximum Soil Thrust		5. TYPE OF REPORT & PERIOD COVERED Final
		6. PERFORMING ORG. REPORT NUMBER RE-556
7. AUTHOR(s) Leslie L. Karafiath		8. CONTRACT OR GRANT NUMBER(s) DAAE07-75-C-0066 Amendments P0004-P0008
9. PERFORMING ORGANIZATION NAME AND ADDRESS Research Department, Grumman Aerospace Corp. Bethpage, New York 11714		10. PROGRAM ELEMENT, PROJECT, TASK AREA & WORK UNIT NUMBERS
11. CONTROLLING OFFICE NAME AND ADDRESS U.S. Army Tank-Automotive Research & Development Command Warren, Michigan 48090		12. REPORT DATE July 1978 13. NUMBER OF PAGES 57
14. MONITORING AGENCY NAME & ADDRESS(if different from Controlling Office)		15. SECURITY CLASS. *(of this report)* Unclassified 15a. DECLASSIFICATION/DOWNGRADING SCHEDULE

16. DISTRIBUTION STATEMENT *(of this Report)*

Approved for public release; distribution unlimited

17. DISTRIBUTION STATEMENT *(of the abstract entered in Block 20, if different from Report)*

18. SUPPLEMENTARY NOTES

19. KEY WORDS *(Continue on reverse side if necessary and identify by block number)*

Acceleration Performance, Center of Gravity, Interface Friction, Passive Resistance, Soil Thrust, Tracked Vehicle, Track-Soil Interaction, Trim Angle.

20. ABSTRACT *(Continue on reverse side if necessary and identify by block number)*

An analytical track-soil interaction model has been developed for the determination of maximum soil thrust. The model assumes rigid track geometry characterized by the dimensions of the main ground contact area and the approach angle. The position of the track is defined by its trim angle and sinkage at the front. Limits of interface stresses are determined by assuming soil failure in either the longitudinal or transverse direction. Within these limits adjustments are made to meet the requirement of moment

DD FORM 1 JAN 73 1473 EDITION OF 1 NOV 65 IS OBSOLETE
S/N 0102-014-6601 |

UNCLASSIFIED

SECURITY CLASSIFICATION OF THIS PAGE *(When Data Entered)*

equilibrium about the CG. The maximum soil thrust is determined by the interface stress distribution that satisfies equilibrium and allows the development of the highest interface friction angle. Results of parametric analyses obtained by the model regarding the effect of track length/width ratios and CG locations on acceleration performance are shown. A semi-rigid track-tire interaction model has also been developed. This model shows that in soft soil the acceleration performance of pin-jointed tracks is governed by the interaction of the soil beneath the last roadwheel and the most rearward track links. Several concepts, aimed at improving the acceleration performance of tracked vehicles, are presented. Turning resistances comprise shear resistances arising at the track-soil interface and passive earth resistances arising at the side faces of tracks. These are analyzed and methods are presented for their computation.